creative commons
COMMONS DEED

저작자표시-비영리-변경금지 2.0 대한민국

이용자는 아래의 조건을 따르는 경우에 한하여 자유롭게

- 이 저작물을 복제, 배포, 전송, 전시, 공연 및 방송할 수 있습니다.

다음과 같은 조건을 따라야 합니다:

저작자표시. 귀하는 원저작자를 표시하여야 합니다.

비영리. 귀하는 이 저작물을 영리 목적으로 이용할 수 없습니다.

변경금지. 귀하는 이 저작물을 개작, 변형 또는 가공할 수 없습니다.

- 귀하는, 이 저작물의 재이용이나 배포의 경우, 이 저작물에 적용된 이용허락조건을 명확하게 나타내어야 합니다.
- 저작권자로부터 별도의 허가를 받으면 이러한 조건들은 적용되지 않습니다.

저작권법에 따른 이용자의 권리는 위의 내용에 의하여 영향을 받지 않습니다.

이것은 이용허락규약(Legal Code)을 이해하기 쉽게 요약한 것입니다.

Disclaimer

dCollection

조선대학교
CHOSUN UNIVERSITY

[UCI]I804:24011-200000368686

February 2021

Ph.D. Dissertation

Design, synthesis and mechanism of action of novel host defense peptides and peptidomimetics with antimicrobial, and anti-inflammatory activities

Graduate School of Chosun University

Department of Biomedical Sciences

Kim Eun Young

조선대학교
CHOSUN UNIVERSITY

Design, synthesis and mechanism of action of novel host defense peptides and peptidomimetics with antimicrobial, and anti-inflammatory activities

항균 및 항염증활성을 가지는 생체 방어 펩타이드 및 펩타이드 모방체의 설계, 합성 및 작용기작

2021년 2월 25일

Graduate School of Chosun University

Department of Biomedical Sciences

Kim Eun Young

조선대학교
CHOSUN UNIVERSITY

Design, synthesis and mechanism of action of novel host defense peptides and peptidomimetics with antimicrobial, and anti-inflammatory activities

Advisor: Prof. Song Yub Shin

This dissertation is submitted to the Graduate School of Chosun University in partial fulfillment of the requirements for the degree of Doctor of Philosophy in Science

October 2020

Graduate School of Chosun University

Department of Biomedical Sciences

Kim Eun Young

조선대학교
CHOSUN UNIVERSITY

Ph. D. Dissertation of

Kim Eun Young is certified by

Chairman (Chosun Univ.) : Prof. Seung Joo Cho .....

Committee Members:

Chosun Univ. : Prof. Sung Tae Yang .....

Chonnam Univ.: Prof. Chul Won Lee .....

Korea Basic Science Institute: Ph.D (P.I.) Jeung Kyu Bang .....

Chosun Univ. : Prof. Song Yub Shin .....

December 2020

Graduate School of Chosun University

조선대학교
CHOSUN UNIVERSITY

CONTENTS

조선대학교
CHOSUN UNIVERSITY

조선대학교
CHOSUN UNIVERSITY

조선대학교
CHOSUN UNIVERSITY

조선대학교
CHOSUN UNIVERSITY

LIST OF TABLES

PART I

PART II

조선대학교
CHOSUN UNIVERSITY

LIST OF FIGURES

PART I

조선대학교
CHOSUN UNIVERSITY

PART II

조선대학교
CHOSUN UNIVERSITY

조선대학교
CHOSUN UNIVERSITY

초 록

항균 및 항염증활성을 가지는 생체 방어 펩타이드 및 펩타이드 모방체의 설계, 합성 및 작용기작

김 은영

지도교수: 신송엽, Ph.D.

의과학과

조선대학교 대학원

PART I

KR-12-a5는 인간 카텔리시딘 LL-37에서 유래된 12-meric α-helical 항균 펩타이드로 항균 및 항 염증 활성을 가진다. 본 연구는 KR-12-a5 보다 높은 세포 선택성(cell selectivity)을 가지며, 항 염증 활성을 유지하는 새로운 α-나선형 항균 펩타이드 개발을 목표로 KR-12-a5의 D-아미노산 치환 유사체(analogs)시리즈를 합성하고 설계하였다. D-아미노산을 KR-12-a5 에게 혼입하면 KR-12-a5에 비해 세포 선택성이 2.6배에서 13.6배까지 향상되는 동시에 항 염증 활성은 유지되었다. 3가지 유사체 중 극성-비극성 표면에 D-아미노산을 가지는(Leu^6), KR-12-a5 ($6-^DL$)가 치료지수(therapeutic index) (세포선택성의 척도임)가 61.2로 가장 높은 세포 선택성을 나타냈다. KR-12-a5 및 그 유사체가 LPS로 자극된 Raw264.7

조선대학교
CHOSUN UNIVERSITY

cell에서 LL-37과 비슷하게, NO 분비가 감소하고 TNF-α, IL-6 및 MCP-1의 발현이 억제되었다. KR-12-a5 및 그 유사체는 임상적으로 분리된 메티실린-저항성 황색포도구균 (MRSA: methicillin-resistant *Staphyllococcus aureus*), 다제내성-녹농균 (multi drug-resistant *Pseudomonas aeruginosa*: MDRPA) 및 반코마이신-저항성 장구균 (vancomycin-resistant *Enterococcus faecium*: VREF)을 포함한 항생제-내성세균에 대해 LL-37 및 Melittin 보다 더 강력한 항균 활성을 나타내었다. 또한 LL-37과 비교하였을 때 KR-12-a5 및 그 유사체가 다제내성-녹농균 (multi drug-resistant *Pseudomonas aeruginosa*: MDRPA)에 대해 기존 항생제(chloramphenicol, ciprofloxacin, 및 oxacillin)과 의 시너지 효과에서 더 큰 활성을 나타내었다. KR-12-a5 및 그 유사체 FICI 범위는 0.25~0.75, LL-37은 0.75~1.5이였다. KR-12-a5 및 그 유사체는 MDRPA에 대해 LL-37보다 강력한 항-바이오 필름 활성을 나타내는 것으로 밝혀졌다. 또한 KR-12-a5 및 그 유사체는 생리적 염(salts) 및 인간 혈청(human serum) 존재에서도 항균 활성을 유지하였다. SYTOX Green uptake 및 막 탈분극 연구에 따르면 KR-12-a5 및 그 유사체는 세포막을 투과하고 막을 손상시켜 미생물 세포를 죽이는 것으로 밝혀졌다. 종합하면 KR-12-a5 및 그 유사체가 항생제 내성 감염을 치료하기 위한 새로운 항균/항 염증제로 더욱 발전할 수 있음을 시사한다.

PART II

TZP4는 항균펩타이드(AMP)의 양친매성 구조를 모방하여 설계된 트리아진

조선대학교
CHOSUN UNIVERSITY

기반 양친매성 중합체이다. TZP4는 메티실린-저항성 황색포도구균 (MRSA: methicillin-resistant *Staphyllococcus aureus*), 다제내성-녹농균 (multi drug-resistant *Pseudomonas aeruginosa*: MDRPA)와 같은 항생제 내성 박테리아에 대해 Melittin과 대항할 정도의 강력한 항균 활성을 나타냈다. TZP4는 단백질 분해에 대한 내성이 높고 약물 내성이 발생하는 경향이 낮았다. 막 탈분극, SYTOX Green uptake, 유세포 분석 및 겔 지연(retardation)의 결과로부터 TZP4의 항균작용 메커니즘은 세포막보다는 세포내 표적이라는 것이 밝혀졌다. 또한 유도성 산화질소 합성 효소(inducible nitric oxide synthase)와 종양 괴사 인자(tumor necrosis factor-α)의 mRNA의 발현을 억제하고 LPS로 자극된 Raw264.7에서 산화질소(NO) 및 TNF-α방출을 억제하였다. BODIPY-TR-cadaverine displacement 및 fluorescein isothiocyanate (FITC)-labelled LPS assay를 통해 TZP4가 LPS에 강하게 결합하고 LPS 올리고머를 분해하는 것을 확인하였다. 유세포 분석으로 TZP4가 Raw264.7 cell에 FITC-라벨된 LPS가 결합하는 것을 억제함을 보여줬다. 이러한 관찰로 TZP4와 LPS에 직접 결합하고 LPS와 $CD14^{+}$ 사이의 상호작용을 억제함으로써 항-내독성 활성을 발휘할 수 있음을 보여줬다. 결론적으로 TZP4는 그람 음성 세균 감염으로 인한 내독성 쇼크 및 패혈증 치료에 유망한 약물 후보임이 입증되었다.

조선대학교
CHOSUN UNIVERSITY

ABSTRACT

Design, synthesis and mechanism action of novel host defense peptide and peptidomimetics with antimicrobial and anti-inflammatory activities

Kim Eun Young

Advisor: Prof. Song Yub Shin

Department of Biomedical sciences

Graduate School of Chosun University

PART I

KR-12-a5 is a 12-meric α-helical antimicrobial peptide (AMP) with dual antimicrobial and anti-inflammatory activities designed from human cathelicidin LL-37. We designed and synthesized a series of D-amino acid-substituted analogs of KR-12-a5 with the aim of developing novel α-helical AMPs that possess higher cell selectivity than KR-12-a5, while maintaining the anti-inflammatory activity. D-amino acid incorporation into KR-12-a5 induced a significant improvement in the cell selectivity by 2.6- to 13.6-fold as compared to KR-12-a5, while maintaining the anti-inflammatory activity. Among the three analogs, KR-12-a5 (6-^{D}L) with D-amino acid in the polar-nonpolar interface (Leu^{6}) showed the highest cell selectivity (therapeutic index: 61.2). Similar to LL-37, KR-12-a5 and its analogs significantly inhibited the expression and secretion of NO, TNF-α, IL-6 and MCP-1 from LPS-stimulated RAW264.7 cells. KR-12-a5 and its analogs showed a more potent antimicrobial activity against antibiotic-resistant bacteria, including clinically isolated MRSA, MDRPA, and VREF than LL-37 and melittin. Furthermore, compared to LL-37, KR-

조선대학교
CHOSUN UNIVERSITY

12-a5 and its analogs showed greater synergistic effects with conventional antibiotics, such as chloramphenicol, ciprofloxacin, and oxacillin against MDRPA; KR-12-a5 and its analogs had a FICI range between 0.25 and 0.5, and LL-37 had a range between 0.75 and 1.5. KR-12-a5 and its analogs were found to be more effective anti-biofilm agents against MDRPA than LL-37. In addition, KR-12-a5 and its analogs maintained antimicrobial activity in physiological salts and human serum. SYTOX Green uptake and membrane depolarization studies revealed that KR-12-a5 and its analogs kills microbial cells by permeabilizing the cell membrane and damaging membrane integrity. Taken together, our results suggest that KR-12-a5 and its analogs can be developed further as novel antimicrobial/anti-inflammatory agents to treat antibiotic-resistant infections.

PART II

TZP4 is a triazine-based amphipathic polymer designed to mimic the amphipathic structure found in antimicrobial peptides. TZP4 showed potent antimicrobial activity comparable to melittin against antibiotic-resistant bacteria, such as methicillin-resistant *Staphylococcus aureus* and multidrug-resistant *Pseudomonas aeruginos*a. TZP4 showed high resistance to proteolytic degradation and low tendency to develop drug resistance. The results from membrane depolarization, SYTOX Green uptake, flow cytometry, and gel retardation revealed that the mechanism of antimicrobial action of TZP4 involved an intracellular target rather than the bacterial cell membrane. Furthermore, TZP4 suppressed the mRNA levels of inducible nitric oxide synthase (iNOS) and tumor necrosis factor-α (TNF-α) and inhibited the release of nitric oxide (NO) and TNF-*α* in lipopolysaccharide (LPS)-stimulated RAW264.7 cells. BODIPY-

조선대학교
CHOSUN UNIVERSITY

TR-cadaverine displacement and dissociation of fluorescein isothiocyanate (FITC)-labelled LPS assays revealed that TZP4 strongly bound to LPS and disaggregated the LPS oligomers. Flow cytometric analysis demonstrated that TZP4 inhibits the binding of FITC-conjugated LPS to RAW264.7 cells. These observations indicate that TZP4 may exert its anti-endotoxic activity by directly binding with LPS and inhibiting the interaction between LPS and $CD14^{+}$ cells. Collectively, TZP4 is a promising drug candidate for the treatment of endotoxic shock and sepsis caused by gram-negative bacterial infections.

PART I

LL-37-derived short antimicrobial peptide KR-12-a5 and its D-amino acid substituted analogs with cell selectivity, anti-biofilm activity, synergistic effect with conventional antibiotics, and anti-inflammatory activity

조선대학교 CHOSUN UNIVERSITY

1. Introduction

Because the increasing emergence of multidrug resistant bacteria is a serious threat to public health, there is an urgent need to develop new antimicrobial agents that are active against bacteria and less likely to induce drug resistance [1–5]. Antimicrobial peptides (AMPs) are attractive candidates as therapeutic agents, because (i) they are capable of killing a broad range of bacteria (including multidrug-resistant strains), fungi, and viruses, and (ii) they rapidly kill pathogens via the nonspecific membranolytic mechanisms, thereby reducing development of the drug resistance [1–5].

LL-37 is the only known member of the cathelicidin family of AMPs in humans [6]. LL-37 is a linear, cationic, α-helical, and amphipathic AMP with 37 residues and a net charge of +6 at physiological pH. It is released from its precursor, hCAP-18, through proteolytic processing by proteinase 3, a serine proteinase secreted from neutrophils [7]. It is active against both Gram-positive and Gram-negative bacteria and some fungi [8].

LL-37 binds to negatively charged bacterial membrane components leading to the formation of pores and cell lysis [9–11]. In addition to exerting antimicrobial activity, it modulates the immune response [12]. LL-37 can neutralize the inflammatory potential of LPS by binding directly to LPS or by preventing the binding of LPS to host cell receptors, thus blocking the cell signaling pathway triggered by TLR ligands [13–15]. These properties make LL-37 an attractive therapeutic agent for Gram-negative bacterial infection and inflammatory disease.

However, the therapeutic application of LL-37 has been hindered by some serious obstacles, such as poor cell selectivity (i.e., the selectivity of bacterial cells over human red blood cells) and high manufacturing costs. Therefore, several studies have attempted to develop truncated LL-37 derivatives with antimicrobial activity equivalent to that of the parent LL-37 [16–20]. KR-12 (residues 18-29 of LL-37: KRIVQRIKDFLR-NH_2) is the smallest peptide of LL-37 possessing antimicrobial activity that was generated from a structure–activity relationship (SAR) study of LL-37 [17]. Recently, we designed a novel KR-12 analog, named KR-12-a5 (KRIVKLILKWLR-NH_2) with a minimal inhibitory concentration (MIC) of 2−8 μM against both Gram-positive and Gram-negative bacteria [19]. KR-12-a5 induced no hemolytic activity at its bacterial MIC, but hemolysis

조선대학교 CHOSUN UNIVERSITY

of 50% at the concentration 96 μM [19]. Such hemolytic activity at high peptide concentrations restricts the therapeutic application of AMPs to topical treatments. In addition to its potent antimicrobial activity, KR-12-a5 significantly inhibited the release of tumor necrosis factor-α (TNF-α) from LPS-stimulated RAW 264.7 cells [19]. These results suggested that KR-12-a5 has the potential for future development as a novel class of antimicrobial and anti-inflammatory therapeutic agents.

In this study, to investigate the effects of single D-amino acid substitutions on KR-12-a5 and to engineer novel, short AMPs possessing higher cell selectivity than KR-12-a5 without loss of anti-inflammatory activity, we synthesized a series of single D-amino acid-substituted analogs based on the α-helical wheel diagram of KR-12-a5. The cell selectivity of KR-12-a5 and its analogs was investigated by examining their antimicrobial activity against Gram-positive and Gram-negative bacterial strains, and their hemolytic activity against human red blood cells. The anti-inflammatory activity of KR-12-a5 and its analogs was established by measuring their ability to suppress the release of NO, TNF-α, interleukin-6 (IL-6), and monocyte chemo-attractant protein-1 (MCP-1) from LPS-stimulated mouse macrophage RAW264.7 cells, as well as to reduce the mRNA levels of TNF-α, inducible nitric oxide synthase (iNOS), IL-6, and MCP-1 in these cells.

The secondary structure of KR-12-a5 and its analogs in the presence of TFE, LPS or SDS was investigated via circular dichroism (CD) spectroscopy. All of the KR-12-a5 analogs showed improved cell selectivity compared to KR-12-a5, without a remarkable loss of anti-inflammatory activity. We evaluated the antimicrobial activity of KR-12-a5 and its analogs against methicillin-resistant *Staphylococcus aureus* (MRSA), multidrug-resistant *Pseudomonas aeruginosa* (MDRPA), and vancomycin-resistant *Enterococcus faecium* (VREF). The stability of KR-12-a5 analogs in physiological salt and human serum was also measured. Concern regarding biofilm-associated infections is growing rapidly worldwide, as biofilms are inherently tolerant and resistant to antimicrobial therapies. Accordingly, the ability of the designed peptides to inhibit the formation of bacterial biofilm against MDRPA was investigated. Furthermore, the synergistic effects of KR-12-a5 and its analogs with three conventional antibiotics with different mechanisms of action against MDRPA were investigated. To understand bacterial killing mechanisms of KR-12-a5 and its analogs,

SYTOX Green uptake and membrane depolarization were studied. Our results will help in the design of novel, short, α-helical AMPs having potent antimicrobial, anti-inflammatory, and anti-biofilm activities as well as synergistic activities with chemical antibiotics without mammalian cell toxicity.

조선대학교
CHOSUN UNIVERSITY

2. Materials and Methods

2.1 Materials

Rink amide-methylbenzhydrylamine (MBHA) resin, 9-fluorenyl-methoxycarbonyl (Fmoc) protected amino acids, and other chemicals and solvents used for peptide synthesis were bought from Novabiochem (La Jolla, CA, USA). Lipopolysaccharide (LPS) purified from *Escherichia coli* O111:B4, 2,2,2-trifluoroethanol (TFE), sodium dodecyl sulfate (SDS), 3-(4,5-dimethylthiazol-2-yl)-2,5-diphenyl-2H-tetrazolium bromide (MTT), egg yolk L-α-phosphatidylcholine (PC), egg yolk L-α-phosphatidyl-DL-glycerol (PG), egg yolk L-α-phosphatidylethanolamine (PE), acrylamide, cholesterol, chloramphenicol, ciprofloxacin, oxacillin, and diSC_3-5 were supplied from Sigma-Aldrich (St. Louis, MO, USA). HyClone Dulbecco's modified Eagle medium (DMEM) and fetal bovine serum (FBS) were obtained from SeouLin Bioscience (Seoul, Korea). The ELISA kits for TNF-α, IL-6, and MCP-1 were procured from R&D Systems (Minneapolis, MN, USA). SYTOX green was purchased from Life Technologies (Eugene, OR, USA). Buffers were prepared using Milli-Q ultrapure water (Merck Millipore, Billerica, MA, USA). All other reagents were of analytical grade.

2.2 Peptide synthesis

The peptides were prepared by the standard Fmoc-based solid-phase synthesis technique on Rink amide MBHA resin. Dicyclohexylcarbodiimide (DCC) and 1-hydroxybenzotriazole (HOBt) were used as coupling reagents, and a 10-fold excess of Fmoc-amino acids was added during every coupling cycle. After cleavage and deprotection with a mixture of TFA/H_2O/thioanisole/phenol/ethanedithiol/triisopropylsilane (81.5:5:5:5:2.5:1, v/v/v/v/v/v) for 2 h at room temperature, the crude peptide was repeatedly extracted with diethyl ether and purified by RP-HPLC (reverse-phase high-performance liquid chromatography) on a preparative Vydac C_{18} column (length: 250 mm, internal diameter: 20 mm, pore size: 300 Å, particle size: 15 mm) using an appropriate 0–90% water/acetonitrile gradient in the presence of 0.05% TFA. The final purity of the peptides (> 95%) was assessed by RP-HPLC on an analytical Vydac C_{18} column (length: 250 mm,

CHOSUN UNIVERSITY

internal diameter: 4.6 mm, pore size: 300 Å, particle size: 5 mm). The success of peptide synthesis was confirmed by analysis using matrix-assisted laser desorption/ionization time-of-flight (MALDI-TOF) mass spectrometry (Shimadzu, Kyoto, Japan).

2.3 Bacterial strains

Three strains of Gram-positive bacteria (*Bacillus subtilis* [KCTC 3068], *Staphylococcus epidermidis* [KCTC 1917], and *Staphylococcus aureus* [KCTC 1621]) and three strains of Gram-negative bacteria (*Escherichia coli* [KCTC 1682], *Pseudomonas aeruginosa* [KCTC 1637], and *Salmonella typhimurium* [KCTC 1926]) were procured from the Korean Collection for Type Cultures (KCTC) of the Korea Research Institute of Bioscience and Biotechnology (KRIBB). Methicillin-resistant *Staphylococcus aureus* strains (MRSA; CCARM 3089, CCARM 3090, and CCARM 3095) and multidrug-resistant *Pseudomonas aeruginosa* strains (MDRPA; CCARM 2095, and CCARM 2109) were obtained from the Culture Collection of Antibiotic-Resistant Microbes (CCARM) of Seoul Women's University in Korea. Vancomycin-resistant *Enterococcus faecium* (VREF; ATCC 51559) was supplied from the American Type Culture Collection (Manassas, VA, USA).

2.4 Antimicrobial assay.

The minimal inhibitory concentrations (MIC) of the peptides against the aforementioned bacterial strains were determined using polystyrene microassay plates (SPL, Pyeongtaek, South Korea). Briefly, microplates inoculated with two-fold serial dilutions of each peptide (starting at 128 μM) in 1% peptone were seeded with a log-phase culture of the target strain diluted in 1% peptone to 2×10^6 CFU/ml. The micro-plates were then incubated at 37 °C for 24 h, and absorbance at 600 nm was measured using a Microplate Autoreader EL 800 (Bio-Tek Instruments, Winooski, VT, USA). MIC values were expressed in micromolar and correspond to the lowest concentration that inhibited the growth of the target microorganism. In order to assess the effects of different salts and human serum on the antimicrobial activity of the peptides, MICs were also determined in the presence of salts. *E. coli* (KCTC 1682) or *S. aureus* (KCTC 1621) at a concentration of 2×10^6 CFU/ml were treated with

조선대학교
CHOSUN UNIVERSITY

peptides in solutions containing physiological concentrations of various salts (150 mM NaCl, or 1 mM $MgCl_2$, or 2.5 mM $CaCl_2$), added to 1% peptone. With the exception of the added salt or serum, MICs were determined using the assay described above.

2.5 Hemolytic activity

Fresh human red blood cells (hRBCs) were washed three times with PBS (35 mM phosphate buffer, 0.15 M NaCl, pH 7.4) and centrifuged for 5 min at 116 × g. A two-fold serial dilution of the peptides in PBS (the concentration test range was 2–512 μM) was added to each well of a 96-well plate (total volume: 100 μl). An equal volume (100 μl) of a 4% w/v hRBC suspension in PBS was added to each well to reach a final volume of 200 μl. The plate was incubated for 1 h at 37 °C, and then the cells were pelleted by centrifugation at 1000 × g for 5 min. The supernatants (100 μl) were transferred to clear 96-well plates. Hemoglobin was detected by measuring absorbance at 414 nm (Molecular Devices, Sunnyvale, CA, USA). The value for "zero hemolysis" was determined using PBS (A_{PBS}), while 100% hemolysis was established using 0.1% (v/v) Triton X-100 (A_{Triton}). The percentage of hemolysis was calculated as follows:

$$hemolysis\ \% = \frac{Asample - APBS}{ATriton\ - APBS} \times 100$$

2.6 Circular dichroism (CD) spectroscopy

All CD measurements were performed on a Jasco J-715 spectropolarimeter (JASCO International Co. Ltd., Tokyo, Japan). The CD spectra at 100 μg/ml peptide concentration in four different environments, i.e., 10 mM sodium phosphate (pH 7.2), 50% TFE, 30 mM (SDS), and 0.1% LPS were recorded from 250 nm to 190 nm, averaged six scans, and collected at 25 °C using the quartz temperature controlled cells with a path length of 0.1 cm. Data were recorded at a scan speed of 20 nm/min, bandwidth of 1.0 nm, 1 s response and 0.1 nm resolution. Following background subtraction, the observed ellipticity, θ (mdeg), was converted to molar ellipticity [θ] (deg·cm^2/dmol) using the following equation: $[\theta]= [\theta]_{obs}(MRW/10cd)$, where $[\theta]_{obs}$ is the experimentally measured ellipticity,

조선대학교 CHOSUN UNIVERSITY

MRW is the mean residue molecular weight of the peptide (molecular weight divided by the number of peptide bond), c is the peptide concentration in mg/ml, and d is the path length of the cell in cm. Assuming a two-state model, the percent α-helix was calculated using the equation, % α-helix = –100 (θ_{222} + 3000)/33000, proposed by McLean et. al [21].

2.7 Intrinsic tryptophan arylamide quenching

Small unilamellar vesicles (SUVs) were prepared for tryptophan fluorescence experiment as described previously [22]. Following chloroform evaporation, the PE-PG (7:3, wt/wt) or PC-cholesterol (10:1, wt/wt) lipids were resuspended in 10 mM Tris-HCl buffer (10 mM Tris [pH 7.4], 150 mM NaCl, 0.1 mM EDTA) by vortexing. The lipid dispersions were sonicated in ice water for 20 min using an ultrasonic cleaner until the solutions clarified. Tryptophan fluorescence spectra were measured using Shimadzu RF-5300PC fluorescence spectrophotometer (Shimadzu Scientific Instruments, Kyoto, Japan). The procedure was performed for each peptide in 10 mM Tris-HCl buffer (pH 7.4) with 500 μM PE-PG or PC-cholesterol lipids. Quenching of fluorescence was accomplished using acrylamide. To reduce the absorbance of acrylamide, Trp was excited at 295 nm [23]. The final concentration of acrylamide was 0.4 M as determined by titrating the 4 M stock solution with liposomes at a lipid/peptide molar ratio of 50:1. The effects of the quenching reagent on peptide fluorescence intensities were assessed by the quenching constant (K_{SV}), which was estimated using the Stern-Volmer equation, $F_0/F = 1 + K_{SV}[Q]$, where F_0 and F are the fluorescence values of the peptide in the absence or the presence of acrylamide, respectively, K_{SV} represents the Stern-Volmer quenching constant, and [Q] represents the concentration of acrylamide [23].

2.8 Cytotoxicity against mammalian cells

Cytotoxicity of peptides against RAW 264.7 and NIH 3T3 cells was determined using the MTT colorimetric assay as previously described [24]. Briefly, the cells were seeded in 96-well plates (2×10^4 cells/well) and cultured for 24 h at 37 °C. Increasing concentrations of the peptides were added and allowed to react with the cells for 48 h, followed by the addition of 20 μl MTT (5 mg/ml in PBS)

조선대학교 CHOSUN UNIVERSITY

for another 4 h at 37 °C. Formazan crystals were dissolved by adding 40 μl of 20% (w/v) SDS containing 0.01 M HCl and incubating for 2 h. Absorbance at 550 nm was measured using a microplate ELISA reader (Molecular Devices, Sunnyvale, CA, USA). Cell survival was calculated using the following formula: survival (%) = (A_{550} of peptide-treated cells / A_{550} of peptide-untreated cells) × 100

2.9 Measurement of NO production from LPS-stimulated RAW264.7 cells

No production from LPS-stimulated RAW264.7 cells was determined as described previously [24]. Briefly, RAW264.7 cells were plated at a density of 5×10^5 cells/ml in 96-well culture plates and stimulated with LPS (20 ng/ml) in the presence or absence of peptides for 24 h. Isolated supernatant fractions were mixed with an equal volume of Griess reagent (1% sulfanilamide, 0.1% naphthylethylenediamine dihydrochloride and 2% phosphoric acid) and incubated at room temperature for 10 min. Nitrite production was quantified by measuring absorbance at 540 nm, and concentrations were determined using a standard curve generated with $NaNO_2$.

2.10 TNF-α release from LPS-stimulated RAW264.7 cells

RAW264.7 cells were seeded in 96-well plates (5×10^4 cells/well) and incubated overnight. Peptides were added and the cultures were incubated at 37 °C for one hour. Subsequently, 20 ng/ml LPS was added and the cells were incubated for another 6 h at 37 °C. Cell supernatants were collected and stored at -20 °C until needed for analysis of cytokine levels. Levels of TNF-α, IL-6 and MCP-1 in the samples were measured by the commercial enzyme-linked immunosorbent assay kit (R&D Systems, Minnespolis, MN, USA) according to the manufacturer's instructions as previously described [24].

2.11 Reverse-transcription polymerase chain reaction (RT-PCR)

RAW264.7 cells were plated at a concentration of 5×10^5 cells/well in six-well plates and incubated overnight. Each peptide was added to the wells. The final concentration of the peptides is

조선대학교 CHOSUN UNIVERSITY

5μM (for NO) or 10μM (for TNF-α, IL-6, and MCP-1). Cells to be used for quantification of iNOS, and TNF-α, IL-6, and MCP-1 were treated for 6 h and 3 h, respectively, with or without (negative control) 20 ng/ml LPS, in the presence or absence of peptide, in DMEM supplemented with 10% bovine serum. The cells were detached from the wells and washed once with PBS. Total RNA was prepared and reverse-transcribed to cDNA using oligo(dT) primers. The primers used were purchased from Bioneer (Seoul, Korea). The cDNA products were amplified in the presence of primers for iNOS (forward, 5'-CTGCAGCACTTGGATCAGGAACCTG-3'; reverse, 5'-GGAGTAGCCTGTGTGCACCTGGAA-3'), TNF-α (forward, 5'-CTGCAGCACTTGGATCAGGAACCTG-3'; reverse, 5'-GGGAGTAGCCTGTG TGCACCTGGAA-3'), IL-6 (forward, 5'-ACAACCACGGCCTTCCCTACTT-3'; reverse, 5'-CACGATTTCCCAGAGAACATGTG-3'), MCP-1 (forward, 5'-ATCCCAATGAGTAGGCTGGAGAGC-3'; reverse, 5'-CAGAAGTGCTTGAGGTGGTTGTG-3'), and GAPDH (forward, 5'-GACATCAAGAAGGTGGTGAA-3'; reverse, 5'-TGTCATACCAGGAAATG AGC-3'). The amplification protocol consisted of an initial denaturation step of 5 min at 94 °C, followed by 30 cycles of denaturation at 94 °C for 1 min, annealing at 55 °C for 1.5 min, and extension at 72 °C for 1 min, and afterwards by a final extension step of 5 min at 72 °C.

2.12 Biofilm assay

Antimicrobial interactions between the peptides and conventional antibiotics were evaluated via the chequerboard assay as described elsewhere [26–28]. Briefly, 2-fold serial dilutions of each antibiotic and each peptide were prepared and added in a 1:1 volume ratio to the wells of a 96-well plate. An equal volume of bacterial solution (100 μl) at ~10^6 CFU/ml was then seeded into each well. The plates were incubated in a shaking incubator at 37 °C and 200 rpm and read after 72 h. Bacterial growth was assessed visually or spectrophotometrically via OD_{600} readings taken by a microplate ELISA reader (Molecular Devices, Sunnyvale, CA, USA). The fractional inhibitory concentration index (FICI) for each drug combination was calculated using the following equation: FICI = [(MIC

조선대학교 CHOSUN UNIVERSITY

of peptide in combination) / (MIC of peptide alone)] + (MIC of antibiotic in combination) / (MIC of antibiotic alone)]. FICI of ≤ 0.5 was interpreted as synergy, 0.5 < FICI ≤ 1.0 as additive, 1.0 < FICI ≤ 4.0 as indifferent, and an FICI > 4.0 as antagonism [26–28].

2.13 Chequerboard assay

Antimicrobial interactions between the peptides and conventional antibiotics were evaluated via the chequerboard assay as described elsewhere [26–28]. Briefly, 2-fold serial dilutions of each antibiotic and each peptide were prepared and added in a 1:1 volume ratio to the wells of a 96-well plate. An equal volume of bacterial solution (100 μl) at ~10^6 CFU/ml was then seeded into each well. The plates were incubated in a shaking incubator at 37 °C and 200 rpm and read after 72 h. Bacterial growth was assessed visually or spectrophotometrically via OD_{600} readings taken by a microplate ELISA reader (Molecular Devices, Sunnyvale, CA, USA). The fractional inhibitory concentration index (FICI) for each drug combination was calculated using the following equation: FICI = [(MIC of peptide in combination) / (MIC of peptide alone)] + (MIC of antibiotic in combination) / (MIC of antibiotic alone)]. FICI of ≤ 0.5 was interpreted as synergy, 0.5 < FICI ≤ 1.0 as additive, 1.0 < FICI ≤ 4.0 as indifferent, and an FICI > 4.0 as antagonism [26–28].

2.14 Cytoplasmic membrane depolarization assay

The effect of peptides on cytoplasmic membrane depolarization was determined using the membrane potential-sensitive dye, $diSC_3$-5, as previously described [14]. Briefly, *S. aureus* (KCTC 1621) grown at 37 °C with agitation to the mid-log phase (OD_{600} = 0.4) was harvested by centrifugation. Cells were washed twice with washing buffer (20 mM glucose and 5 mM HEPES, pH 7.4) and resuspended to an OD_{600} of 0.05 in the same buffer. The cell suspension was incubated with 20 nM $diSC_3$-5 until a stable fluorescence value was achieved, implying the full incorporation of the dye into the bacterial membrane. Membrane depolarization was monitored based on the changes in the intensity of the fluorescence emitted from the $diSC_3$-5 (excitation λ = 622 nm, emission λ = 670

조선대학교
CHOSUN UNIVERSITY

nm) after peptide addition. The membrane potential was fully abolished by adding gramicidin D at a final concentration of 0.2 nM.

2.15 SYTOX green uptake assay

The effect of the peptides on bacterial membrane permeabilization was evaluated using the SYTOX green uptake assay as previously described [24,31]. *S. aureus* (KCTC 1621) in mid-logarithmic phase was collected and washed 3 times with a buffer containing 5 mM HEPES (pH 7.4) and 20 mM glucose. Following washing, the pelleted bacteria were re-suspended in a buffer containing 5 mM HEPES (pH 7.4), 20 mM glucose, and 100 mM KCl. S. *aureus* suspensions of 1×10^6 CFU/ml were prepared and mixed with 0.5 μM SYTOX Green for 15 min in the dark. After the addition of peptides to a final concentration equal to 2 × MIC, the uptake of SYTOX Green was monitored using a Shimadzu RF-5300PC fluorescence spectrophotometer (Shimadzu Scientific Instruments, Kyoto, Japan), with filter wavelengths of 485 and 520 nm for excitation and emission, respectively. This is possible because the cationic dye, which can only cross compromised membranes, binds to intracellular DNA and this interaction results in a significant increase of fluorescence intensity. Bacteria treated with melittin (a toxin from bee venom) or LL-37 were used as positive controls to provide maximal permeabilization values.

2.17 Statistical analysis

All results are presented as averages of values derived from three independent experiments, with triplicates used in each experiment. Error bars represent the mean ± standard deviation of the mean. The statistical significance of differences between samples and respective controls (no added antimicrobial agent) were determined by one-way analysis of variance (ANOVA) with Bonferroni's post-test method using Sigmaplot v12.0 (Systat Software Inc., San Jose, CA, USA). Differences with $P < 0.001$ were considered statistically significant.

조선대학교
CHOSUN UNIVERSITY

3. Results

3.1 Peptide design and synthesis

As shown in the α-helical wheel projection of KR-12-a5, the positively charged amino acid residues (Lys and Arg) of KR-12-a5 are located on one side, whereas the hydrophobic amino acid residues (Val, Leu, Ile, and Trp) are on the other side of the helical axis, presenting a perfect amphipathic helix structure (Fig. 1). To investigate the effects on cell selectivity of single D-amino acid substitutions into the polar (hydrophilic) face, nonpolar (hydrophobic) face, or polar-nonpolar (hydrophilic-hydrophobic) interface of the amphipathic *α*-helical AMP KR-12-a5, we designed and synthesized three KR-12-a5 analogs. KR-12-a5(5-^{D}K) and KR-12-a5(7-^{D}L) were designed by introducing D-Lys and D-Leu into the Lys^{5} and Ile^{7} in the central position of the polar and non-polar face of KR-12-a5, respectively. KR-12-a5(6-^{D}L) was designed by substituting D-Leu for Leu^{6} in the polar-nonpolar interface of KR-12-a5. In this study, we aimed to create KR-12-a5 analogs with improved cell selectivity without loss of anti-inflammatory activity, using a single D-amino acid substitution. The structures and molecular weights of KR-12-a5 and its D-amino acid-substituted analogs were verified via MALDI-TOF MS. The theoretically calculated and measured molecular weight of each peptide is summarized in Table 1. The measured molecular weight value of all peptides matched closely with the theoretical value, indicating that the peptides were successfully synthesized.

3.2 Hydrophobicity

RP-HPLC retention behaviors of peptides are highly sensitive to their conformational status upon interacting with the hydrophobic environment of the column matrix, and are widely utilized to determine the relative hydrophobicity of peptides [32]. In this study, the hydrophobicity of our peptides was determined using analytical RP-HPLC. The relative hydrophobicity of KR-12-a5 and its analogs are in the order of KR-12-a5 > KR-12-a5(5-^{D}K) > KR-12-a5(7-^{D}L) = KR-12-a5(6-^{D}L) (Table 1).

CHOSUN UNIVERSITY

3.3 Antimicrobial activity

The antimicrobial activity of the peptides against three Gram-positive and three Gram-negative bacterial strains was tested by determining the minimal inhibitory concentration (MIC), as summarized in Table 2. The potency of antimicrobial activity was ranked according to the geometric means of the MICs as follows: KR-12-a5(6-^{D}L) > KR-12-a5(7-^{D}L) > KR-12-a5(5-^{D}K) > KR-12-a5.

3.4 Hemolytic activity

The ability of the peptides to induce hemolysis of human erythrocytes was examined as a measure of peptide toxicity to mammalian cells (Fig. 2). For the measurement of the hemolytic activity of the peptides, we determined the minimal hemolytic concentration (MHC), defined as the lowest peptide concentration that produces 10% hemolysis against human red blood cells (Table 3). The potency of the hemolytic activity of the peptides was ranked according to the MHC, as follows: KR-12-a5 > KR-12-a5(5-^{D}K) > KR-12-a5(7-^{D}L) > KR-12-a5(6-^{D}L) (Fig. 2 and Table 3).

3.5 Cell selectivity

The therapeutic potential of antimicrobial agents is dependent on their selectivity to kill bacteria as opposed to normal mammalian cells. The cell selectivity of the peptides is expressed as the therapeutic index (TI) = MHC/GM, where MHC is the peptide concentration needed to reach 10% lysis of human red blood cells, while GM is the geometric mean of MICs toward all tested bacteria (Table 3). The TI is an important parameter used to evaluate the balance between the toxic and the desired effect of a drug [33–35]. Thus, larger TI values indicate better cell selectivity. KR-12-a5(5-^{D}K), KR-12-a5(6-^{D}L), and KR-12-a5(7-^{D}L) and showed an increase in TI value of approximately 3.8-, 13.9- and 6.8-fold, respectively, compared to KR-12-a5. Among the D-amino acid substituted analogs, KR-12-a5(6-^{D}L) with the D-amino acid in the polar-nonpolar interface, show the highest TI of 61.2.

조선대학교
CHOSUN UNIVERSITY

3.6 Secondary structure by CD spectra

The secondary structures of the peptides in membrane-mimetic environments were investigated using CD spectroscopy. The CD spectra of the peptides in 10 mM sodium phosphate buffer, pH 7.4 (an aqueous environment), 50% TFE (mimicking the hydrophobic environment of the microbial membrane), 30 mM SDS (mimicking the negatively charged microbial membrane environment), or 0.1% LPS (mimicking the microbial outer surface environment) are shown in Fig. 3. All peptides adopted a clear random coil conformation in aqueous buffer. In contrast, the CD spectra of all peptides show a strong, positive peak at 192 nm and two negative peaks at 208 and 222 nm in TFE, SDS, and LPS solutions, which indicates a predominantly α-helical conformation. The α-helical content (%) of each peptide in 50% TFE, 30mM SDS, and 0.1% LPS is shown in Table 4. KR-12-a5, KR-12-a5(5-^{D}K), and KR-12-a5(6-^{D}L) showed nearly identical α-helical content in all three solutions. However, the helical content of KR-12-a5(7-^{D}L) was consistently lower than that of KR-12-a5, KR-12-a5(5-^{D}K), and KR-12-a5(6-^{D}L).

3.7 Quenching of tryptophan fluorescence with acrylamide

To investigate the relative extent of peptide burial in liposomes and the lipid specificity of the peptide–liposome interaction, we examined the effect of acrylamide, a water-soluble neutral quencher of tryptophan fluorescence. Acrylamide is useful as a quenching agent because it does not interact with the head group of negatively charged phospholipids. The Stern–Volmer plots for the quenching of tryptophan by acrylamide in Tris–HCl buffer, in the presence of PE/PG (7:3, w/w) vesicles or in the presence of PC/cholesterol (10:1, w/w) vesicles, are depicted in Fig. 4. The tryptophan fluorescence for all peptides decreased in a concentration-dependent manner on the addition of acrylamide. In negatively charged PE/PG (7:3, w/w) liposomes, KR-12-a5 and its analogs showed similar slopes and Ksv. In contrast, in zwitterionic PC/cholesterol (10:1, w/w) liposomes, the KR-12-a5 analogs demonstrated slightly higher slopes and larger Ksv than KR-12-a5, suggesting that the Trp residue of all KR-12-a5 analogs is less anchored within the hydrophobic core of the

조선대학교
CHOSUN UNIVERSITY

zwitterionic phospholipids compared to the Trp residue of KR-12-a5 (Fig. 4 and Table 5). This was in agreement with the observation that all KR-12-a5 analogs are less hemolytic than KR-12-a5.

3.8 Cytotoxicity of peptides against mammalian cells

To assess the cytotoxicity of the peptides against mammalian cells, mouse macrophage RAW264.7 cells and mouse NIH-3T3 fibroblast cells were treated with different concentrations of each peptide (0–128 μM). The viability of RAW264.7 and NIH-3T3 cells was subsequently evaluated using the MTT assay, which is based on the reduction of 3-(4,5-dimethyl-2-thiazolyl)-2,5-diphenyl-2H-tetrazolium bromide into formazan dye by the mitochondria of living cells. As illustrated in Fig. 5, none of the peptides affected the viability of RAW264.7 and NIH-3T3 cells at concentrations as high as 128 μM.

3.9 Inhibitory effect of peptides on LPS-stimulated NO and cytokine release

To assess the effects of the peptides on the release of NO TNF-α, IL-6, and MCP-1 from LPS-stimulated RAW264.7 cells, cells were treated with or without 20 ng/ml LPS in the presence of the peptides. NO production can be determined using the Griess method that detects nitrite ion (NO_2^-) accumulation in culture media. The release of TNF-α, IL-6, and MCP-1 was assayed with an ELISA kit. Although weak compared to LL-37, KR-12-a5 and its analogs significantly blocked the release of NO, TNF-α, IL-6, and MCP-1 from LPS-stimulated RAW264.7 cells at both 10 and 20 μM (Fig. 6).

3.10 Inhibition of the expression of iNOS, TNF-α, IL-6 and MCP-1 in LPS-stimulated RAW264.7 cells.

LPS induces the expression of iNOS, TNF-α, IL-6 and MCP-1 in LPS-stimulated RAW264.7 cells, which correlates with NO, TNF-α, IL-6 and MCP-1 release. Therefore, the effects of the peptides on LPS-induced expression of iNOS, TNF-α, IL-6, and MCP-1 mRNA were examined via RT-PCR (Fig. 7). Similar to LL-37, KR-12-a5 and its analogs significantly reduced the expression of iNOS,

CHOSUN UNIVERSITY

TNF-α, IL-6, and MCP-1 at 5 or 10 μM. These data are in agreement with the observed inhibition of NO, TNF-α, IL-6, and MCP-1 production by the peptides.

3.11 Antimicrobial activity against antibiotic-resistant bacteria

To prove the efficacy of KR-12-a5 and its analogs against multidrug-resistant bacteria, we screened their antimicrobial activity against three MRSA strains (CCARM 3089, CCARM 3090, and CCARM 3095), two MDRPA strains (CCARM 2109, and CCARM 2095) and a VREF strain (ATCC 51559). KR-12-a5 and its analogs show higher (2- to 4-fold) antimicrobial activity against all tested antibiotic-resistant bacterial strains than LL-37 and melittin (Table 6). This result indicates that KR-12-a5 and its analogs may represent a potential lead structure of antimicrobial agents effective against antibiotic-resistant bacteria.

3.12 Salt and serum stability

To investigate the effects of salts on antimicrobial activity, KR-12-a5 and its analogs were tested for antimicrobial activity against *E. coli* and *S. aureus* in the presence of different salts at physiological concentrations (i.e., 150 mM NaCl, 4.5 mM KCl, 6 μM NH_4Cl, 1 mM $MgCl_2$, or 2.5 mM $CaCl_2$). As shown in Table 7, the effect varied depending on the peptide and the salt, with some peptide/salt combinations showing activity similar to that of the peptide in the absence of salt, and others presenting a 2- to 4-fold decrease in activity. KR-12-a5 and its analogs showed a similar stability in the presence of physiological salts compared to LL-37. We also treated the bacteria with LL-37, KR-12-a5 and its analogs in the presence of 20% human serum. All peptides retained their antimicrobial activity against *E. coli* in 20% human serum, but showed a 2- to 8-fold decrease in antimicrobial activity against *S. aureus.*

3.13 Biofilm inhibition

The ability of the peptides to inhibit the formation of bacterial biofilm was investigated against MDRPA (CCARM 2095). KR-12-a5 and its analogs were found to be effective inhibitors in MDRPA

조선대학교 CHOSUN UNIVERSITY

biofilm formation. The IC_{90} values (i.e., the concentrations of the compounds that inhibit biofilm development by 90%) of KR-12-a5, KR-12-a5(5-^{D}K), KR-12-a5(6-^{D}L), and KR-12-a5(7-^{D}L) against MDRPA biofilm formation were found to be 16, 8, 16, and 8 μM, respectively (Fig. 8). However, the parental peptide, LL-37, did not show a significant anti-biofilm activity until 64 μM. Thus, the ability of KR-12-a5 and its analogs to inhibit biofilm formation makes them promising anti-biofilm agents.

3.14 Synergy with conventional antibiotics

The synergistic effects of the KR-12-a5 analogs with three conventional antibiotics, chloramphenicol, ciprofloxacin, and oxacillin were also investigated against MDRPA by using a checkerboard assay [26–28]. The FICI data of the peptide combinations are summarized in Table 8. KR-12-a5 and its analogs showed a remarkable synergy with all three antibiotics against MDRPA, with FICI values from 0.3125 to 0.5. However, LL-37 showed an additive effect with chloramphenicol and ciprofloxacin, with FICI values of 0.75 and 1.0, respectively, and an indifferent effect with oxacillin with a FICI value of 1.50.

3.15 Mechanism of antimicrobial action

The mechanism of antimicrobial action of KR-12-a5 and its analogs was assessed by SYTOX Green uptake and membrane depolarization. First, we assessed the ability of the peptides to affect bacterial membrane permeability at 2 × MIC by monitoring the intracellular influx of SYTOX Green, a fluorescent nucleic acid stain. The SYTOX Green, DNA-binding dye becomes fluorescent when bound to nucleic acids, and only enters cells with a compromised plasma membrane [30]. The pore-forming or membrane-disrupting AMPs, LL-37 and melittin were used as positive control peptides [11, 36]. The intracellular-targeting AMP, buforin-2 was used as a negative control peptide [37]. Like LL-37 and melittin, KR-12-a5 and its analogs were able to permeate the membrane of *S. aureus*, as indicated by the increase in fluorescence of samples treated with peptides compared to that of the negative controls (no peptide). They induced a rapid permeabilization with maximum SYTOX Green

조선대학교
CHOSUN UNIVERSITY

levels reached within 4 min (Fig. 9). However, buforin-2 permeabilized poorly with a very weak SYTOX Green fluorescence signal (Fig. 9). We also applied a membrane depolarization assay to examine the effects of KR-12-a5 and its analogs on the potential of the cytoplasmic membrane of *S. aureus*. The $diSC_3$-5 dye concentrates in the cytoplasmic membrane in a membrane potential-dependent manner, which results in the self-quenching of its fluorescence. Upon permeabilization and disruption of the cytoplasmic membrane, the membrane potential is dissipated and $diSC_3$-5 is released into the medium, causing an increase in fluorescence. The membrane depolarization of *S. aureus* was also analyzed by monitoring the increase in fluorescence of $diSC_3$-5 (Fig. 10). Except for buforin-2, all peptides quickly induced complete membrane depolarization against *S. aureus* at 2 × MIC. KR-12-a5 and its analogs caused depolarization of the cytoplasmic membrane that was faster than that seen with LL-37. These results with SYTOX Green uptake and membrane depolarization indicate that KR-12-a5 and its analogs kill microorganisms by a membrane damage mechanism of pore formation or membrane disruption.

조선대학교 CHOSUN UNIVERSITY

4. Discussion

In this study, we aimed to develop novel, short, α-helical AMPs that possess higher cell selectivity than KR-12-a5 does, while maintaining anti-inflammatory activity, by using D-amino acid incorporation. D-amino acid incorporation into KR-12-a5 induced a significant improvement in the cell selectivity by 2.6- to 13.6-fold compared to KR-12-a5. Among the three analogs, KR-12-a5(6-^{D}L) with D-amino acid in the polar-nonpolar interface (Leu^{6}) showed the highest cell selectivity [therapeutic index (TI) = 61.2)]. KR-12-a5(6-^{D}L) induced minimal hemolysis (less than 10%) even at a high concentration of 200 μM. The cell selectivity of antimicrobial agents represented as TI values can be increased via one of the following three ways: (i) increasing antimicrobial activity, (ii) decreasing hemolytic activity while maintaining antimicrobial activity, or (iii) a combination of both increasing antimicrobial activity and decreasing hemolytic activity. The improvement in cell selectivity of all of the KR-12-a5 analogs is due to their decreasing hemolytic activity while maintaining antimicrobial activity. SAR studies using different kinds of natural and synthetic α-helical AMPs revealed that the hydrophobicity of α-helical AMPs is closely related to the hemolytic activity. Therefore, the reduced hemolytic activity of all of the KR-12-a5 analogs is due to their reduced hydrophobicity. The retention time in analytical RP-HPLC indicated that all of the KR-12-a5 analogs were less hydrophobic than KR-12-a5 (Table 1). Among the KR-12-a5 analogs, L6-D possessing the lowest hemolytic activity, showed the lowest hydrophobicity. Because KR-12-a5 and its analogs contain one tryptophan in position 10, we investigated the relative extent of peptide burial in bacterial outer membrane-mimicking PE/PG (7:3. v/v) vesicles and mammalian outer membrane-mimicking PC/cholesterol (10:1, v/v) vesicles, using a tryptophan fluorescence acrylamide quenching experiment. This experiment showed that the tryptophan residue of each KR-12-a5 analog was inserted less into the nonpolar environment of the PC/cholesterol (10:1, v/v) vesicles than that of KR-12-a5. This result is consistent with the reduced hemolytic activity of the KR-12-a5 analogs. Furthermore, our results are in agreement with previous reports showing that incorporation of D-amino acids into cytolytic AMPs such as pardaxin, melittin, or synthetic peptides causes (i) minimizing mammalian cell toxicity while retaining antimicrobial activity and ability to permeate

조선대학교 CHOSUN UNIVERSITY

anionic outer membranes, and (ii) increases the resistance of diastereomers to human serum inactivation [38-40].

LPS is a major component of the outer membrane of Gram-negative bacteria. LPS can be released during bacterial cell division, cell death, or especially, after antibiotic treatment of Gram-negative bacterial infections. LPS is also known as an endotoxin, a potent inducer of the innate immune system in humans [41–44]. Once LPS is released into the blood system, it causes monocytic and phagocytic cells to produce large amounts of proinflammatory cytokines, including TNF-α, IL-6, IL-β, and others. The overexpression of these cytokines can cause multiple organ damage, such as septic shock syndrome [41–44]. Septic shock is the major cause of mortality in intensive care units accounting for 600,000 deaths every year in the United States alone [45]. For this reason, novel antimicrobial agents should show dual antimicrobial and LPS-neutralizing activities. Recent studies have found that some AMPs, such as LL-37, not only show a broad antimicrobial spectrum but also inhibit the release of inflammatory cytokines by direct LPS-binding or modulating signaling pathways on macrophages to induce anti-inflammatory effects [46–50]. Like LL-37, KR-12-a5 and its analogs significantly inhibited the secretion of pro-inflammatory mediators and their mRNA expression in LPS-stimulated RAW264.7 cells at 5–20 μM. Collectively, all of the KR-12-a5 analogs showed improved cell selectivity compared to KR-12-a5 without loss of anti-inflammatory activity.

A major limitation of the use of natural AMPs for systemic applications is their possible inactivation by physiological concentrations of salts [51,52]. To be effective in clinical applications, AMPs must retain the ability to kill microbes in physiological concentrations of salts. Hence, in order to examine the effect of salts on antimicrobial activity of the KR-12-a5 analogs, we treated *E. coli* and *S. aureus* with KR-12-a5 and its analogs in the presence of physiological concentrations of salts. Interestingly, the monovalent (Na^+, K^+, and NH_4^+) and divalent (Mg^{2+} and Ca^{2+}) cations showed little or no effect on the MIC values of KR-12-a5 and its analogs. Generally, KR-12-a5 and its analogs showed similar stability in the presence of physiological salts as LL-37.

In recent years, severe infections caused by multidrug-resistant bacteria have become a major challenge for conventional antibiotic treatments. Hence, to probe the efficacy of KR-12-a5 and its analogs against multidrug-resistant bacteria, their antimicrobial activities against MRSA, MDRPA,

조선대학교 CHOSUN UNIVERSITY

and VREF strains were tested. Interestingly, KR-12-a5 and its analogs showed greater antimicrobial activity against MRSA, MDRPA, and VREF strains than LL-37 and melittin. This result indicates that KR-12-a5 and its analogs may represent potential peptide-antibiotic lead structures against drug-resistant bacteria.

In recent years, severe infections caused by multidrug-resistant bacteria have become a major challenge for conventional antibiotic treatments. Hence, to probe the efficacy of KR-12-a5 and its analogs against multidrug-resistant bacteria, their antimicrobial activities against MRSA, MDRPA, and VREF strains were tested. Interestingly, KR-12-a5 and its analogs showed greater antimicrobial activity against MRSA, MDRPA, and VREF strains than LL-37 and melittin. This result indicates that KR-12-a5 and its analogs may represent potential peptide-antibiotic lead structures against drug-resistant bacteria.

The control of bacterial infections becomes very challenging if pathogenic bacteria are organized as a biofilm community. Conventional antibiotics that are effective against planktonic bacterial cells might fail in controlling the pathogens organized in such communities, since microbial biofilms are intrinsically resistant to antibiotics [53]. In particular, biofilm infection by biofilm-forming MDRPA in the lungs of cystic fibrosis (CF) patients is the leading cause of their morbidity and can lead to functional failure of this organ [54]. Hence, there is an urgent need to identify compounds that effectively clear biofilm-related infections. Some cathelicidin-derived AMPs such as LL-37, SMAP-29, BMAP-28, and BMAP-27 significantly reduced biofilm formation by *P. aeruginosa* or *S. maltophilia* strains [55, 56]. Thus, we evaluated the anti-biofilm ability of KR-12-a5 and its analogs against MDRPA biofilm formation. KR-12-a5 and its analogs showed a 4- to 8-fold increased anti-biofilm activity against MDRPA compared to LL-37. KR-12-a5 and its analogs thus be useful not only as lead compounds for the development of novel antibiotics but also for compounds that may counteract bacterial biofilm formation, thus finding application as an early prophylactic and therapeutic treatment of CF lung disease.

Combination antibiotic therapy is sometimes used for the treatment of routine bacterial infections [57,58]. Thus, it is reasonable to propose a combination therapy utilizing AMPs and conventional antibiotics, because the mechanism of action of AMPs is dramatically different from that of

조선대학교 CHOSUN UNIVERSITY

conventional antibiotics. In combining conventional antibiotics with AMPs, synergy occurs because there is better intracellular uptake of conventional antibiotics that subsequently have bactericidal effects [59,60]. Therefore, we investigated the synergistic effects of combining the peptides with conventional antibiotics against MDRPA, which was already resistant to these antibiotics with an MIC range of 512 to 1024 μM. We used three conventional antibiotics with different mechanisms of activity, namely chloramphenicol (a protein synthesis inhibitor), ciprofloxacin (a DNA gyrase inhibitor), and oxacillin (a cell wall synthesis inhibitor). The site of action of oxacillin is outside of the cytoplasmic membrane, while ciprofloxacin and chloramphenicol act intracellularly. KR-12-a5 and its analogs showed more potent synergistic activity with all three antibiotics against MDRPA, with a range of FICIs between 0.3125 and 0.5, compared to LL-37, with a range of FICIs between 0.75 and 1.5. Thus, KR-12-a5 and its analogs showed greater synergistic effects with chloramphenicol, ciprofloxacin, or oxacillin against MDRPA than LL-37 did. Taken together, the combination therapies of KR-12-a5 and its analogs and conventional antibiotics were evaluated to improve the effectiveness of the antibiotics and prevent or delay the development of antibiotic resistance.

Many α-helical AMPs permeabilize the lipid bilayer of the cytoplasmic membrane, which results in the dissipation of transmembrane potential and subsequent cell death [61,62]. KR-12-a5 and its analogs adopted a typical α-helical conformation in membrane-mimicking environments, such as TFE, SDS, and LPS solutions, suggesting that these peptides exert antimicrobial activity via the permeabilization of the bacterial membrane. To test this hypothesis, the SYTOX Green membrane-permeability assay was performed, which depends on the fact that SYTOX Green dye can only cross compromised membranes, thus, its accumulation inside bacterial cells indicates cytoplasmic membrane disruption. As was also the case with melittin and LL-37, KR-12-a5 and its analogs induced a rapid permeabilization with a maximum SYTOX Green accumulation reached at 2 × MIC within 4 min. Similar to melittin and LL-37, KR-12-a5 and its analogs induced nearly complete depolarization of *S. aureus* membranes at 2 × MIC. Taken together, these results indicate that KR-

12-a5 and its analogs kill bacterial cells most likely by membrane disruption/permeabilization, although the involvement of other mechanisms cannot be ruled out.

조선대학교
CHOSUN UNIVERSITY

5. Conclusion

In the present study, we succeeded in engineering three KR-12-a5 analogs possessing improved cell selectivity compared to KR-12-a5 without loss of anti-inflammatory activity by incorporating a single D-amino acid into LL-37-derived 12-meric AMP (KR-12-a5). KR-12-a5 and its analogs proved to be more effective than LL-37 in terms of, (i) antimicrobial activity against antibiotic-resistant bacteria, including MRSA, MDRPA, and VREF; (ii) anti-biofilm activity against MDRPA; (iii) synergy with chloramphenicol, ciprofloxacin, and oxacillin against MDRPA; and (iv) resistance to physiological salts. SYTOX Green uptake and membrane depolarization experiments revealed that KR-12-a5 and its analogs kill microbial cells by inducing loss of cytoplasmic membrane potential, permeabilization, and disruption. Collectively, our results suggest that KR-12-a5 and its analogs can be developed into novel antimicrobial/anti-inflammatory agents.

조선대학교
CHOSUN UNIVERSITY

Table 1. Amino acid sequence and physicochemical properties of KR-12-a5 and its analogs.

Peptides	Amino acid sequences	Molecular mass (Da)		Net charge	R^t (min)[b]
		Calculated	Observed[a]		
KR-12-a5	KRIVKLILKWLR-NH_2	1565.1	1564.8	+6	23.5
KR-12-a5(5-^{D}K)	KRIV**K**LILKWLR-NH_2	1565.1	1564.8	+6	22.1
KR-12-a5(6-^{D}L)	KRIVK**L**ILKWLR-NH_2	1565.1	1564.7	+6	21.8
KR-12-a5(7-^{D}L)	KRIVKL**L**LKWLR-NH_2	1565.1	1564.8	+6	21.8

The substituted D-amino acids are shown in bold and underlined.

[a] Molecular mass was determined using MALDI-TOF-MS.

[b] Retention time (R^t) was measured using a C_{18} reversed-phase analytical HPLC column (5 m; 4.6 mm × 250 mm; Vydac). Peptides were eluted for 60 min, by using a linear gradient of 0–90% (v/v) acetonitrile in water containing 0.05% (v/v) TFA.

조선대학교
CHOSUN UNIVERSITY

Table 2. MICs of KR-12-a5 and its analogs against bacterial strains.

Peptides	Minimal inhibitory concentration (MIC)[a] (μM)					
	E. coli [KCTC 1682]	*P. aeruginosa* [KCTC 1637]	*S. typhimurium* [KCTC 1926]	*B. subtilis* [KCTC 3068]	*S. epidermidis* [KCTC 1917]	*S. aureus* [KCTC1621]
KR-12-a5	8	8	2	8	4	4
KR-12-a5(5-^{D}K)	4	8	2	8	4	2
KR-12-a5(6-^{D}L)	4	4	2	4	4	2
KR-12-a5(7-^{D}L)	4	8	2	2	4	2

[a] MIC was determined as the lowest concentration of peptide that caused 100 % inhibition of microbial growth.

조선대학교
CHOSUN UNIVERSITY

Table 3. Amino acid sequence and physicochemical properties of KR-12-a5 and its analogs.

Peptides	Amino acid sequences	Molecular mass (Da)		Net charge	R^t (min)[b]
		Calculated	Observed[a]		
KR-12-a5	KRIVKLILKWLR-NH_2	1565.1	1564.8	+6	23.5
KR-12-a5(5-^{D}K)	KRIV**K**LILKWLR-NH_2	1565.1	1564.8	+6	22.1
KR-12-a5(6-^{D}L)	KRIVK**L**ILKWLR-NH_2	1565.1	1564.7	+6	21.8
KR-12-a5(7-^{D}L)	KRIVKL**L**LKWLR-NH_2	1565.1	1564.8	+6	21.8

The substituted D-amino acids are shown in bold and underlined.

[a] Molecular mass was determined using MALDI-TOF-MS.

[b] Retention time (R^t) was measured using a C_{18} reversed-phase analytical HPLC column (5 m; 4.6 mm × 250 mm; Vydac). Peptides were eluted for 60 min, by using a linear gradient of 0–90% (v/v) acetonitrile in water containing 0.05% (v/v) TFA.

조선대학교
CHOSUN UNIVERSITY

Table 4. Mean residual ellipticity at 222 nm ($[\theta]_{222}$) and percent α-helical contents of KR-12-a5 and its analogs in aqueous buffer, 50% TFE (v/v), 30 mM SDS and 0.1 % LPS.

Peptide	Buffer		50% TFE		30mM SDS		0.1% LPS	
	$[\theta]_{222}$	% α-helix	$[\theta]_{222}$	% α-helix	$[\theta]_{222}$	% α-helix	$[\theta]_{222}$	% α-helix
KR-12-a5	-2536.9	rc	-14533.3	34.9	-14735.5	35.6	-10254.6	27.5
KR-12-a5(5-^{D}K)	-2409.4	rc	-15735.3	38.6	-14274.8	34.2	-10168.4	21.9
KR-12-a5(6-^{D}L)	-2270.6	rc	-15216.6	37.0	-14786.1	35.7	-9190.0	18.8
KR-12-a5(7-^{D}L)	-1888.1	rc	-11411.4	25.5	-12662.2	29.3	-8641.8	17.1

% α-helix = -100 ($[\theta]_{222}$ + 3000)/33000. rc means random coli.

조선대학교
CHOSUN UNIVERSITY

Table 5. K_{sv} values of Trp residues of KR-12-a5 and its analogs in buffer, PE/PG, and PC/cholesterol vesicles.

Peptide	K_{sv}[a](M^{-1})		
	Tris-HCl buffer	EYPE/EYPG(7:3. v/v) vesicles	EYPC/cholesterol(10:1, v/v) vesicles
KR-12-a5	5.95	1.12	1.66
KR-12-a5(5-^{D}K)	7.56	1.02	2.21
KR-12-a5(6-^{D}L)	7.31	0.97	2.90
KR-12-a5(7-^{D}L)	7.46	1.01	2.98

[a] The Stern-Vollmer constant K_{SV} was calculated by the Stern-Vollmer equation, $F_0/F = 1 + K_{SV}$ (Q), where Q is the concentration of the quencher (acrylamide).
Concentrations of the quencher were increased from 0.01 to 0.18M.
A smaller K_{SV} value reflects a more protected Trp residues.

조선대학교
CHOSUN UNIVERSITY

Table 6. Antimicrobial activities of the peptides against antibiotic-resistant bacterial strains.

Microorganisms	MIC (μM)					
	KR-12-a5	KR-12-a5(5-^{D}K)	KR-12-a5(6-^{D}L)	KR-12-a5(7-^{D}L)	LL-37	Melittin
MRSA[a]						
CCARM 3089	4	4	4	4	32	8
CCARM 3090	8	4	4	4	16	8
CCARM 3095	4	4	4	4	8	8
MDRPA[b]						
CCARM 2095	16	8	8	8	8	16
CCARM 2109	8	4	4	4	16	16
VREF[c]						
ATCC 51559	4	4	4	4	16	16

[a] MRSA: methicillin-resistant *Staphylococcus aureus*
[b] MDRPA: multidrug-resistant *Pseudomonas aeruginosa*
[c] VREF: vancomycin-resistant *Enterococcus faecium*

조선대학교
CHOSUN UNIVERSITY

Table .7 MIC values of the peptides in the presence of physiological salts and human serum (20%) against *E. coli* and *S. aureus*.

Peptides	Control	150 mM NaCl	4.5 mM KCl	6 μM NH_4Cl	1 mM $MgCl_2$	2.5 mM $CaCl_2$	20% Human Serum
MIC (μM) against *E. coli* (KCTC 1682)							
KR-12-a5	8	8	8	8	8	8	8
KR-12-a5(5-^{D}K)	4	4	4	4	8	8	4
KR-12-a5(6-^{D}L)	4	4	4	4	4	16	8
KR-12-a5(7-^{D}L)	4	4	4	4	8	16	4
LL-37	8	8	8	8	16	32	16
MIC (μM) against *S. aureus* (KCTC 1621)							
KR-12-a5	4	2	2	2	8	2	8
KR-12-a5(5-^{D}K)	2	2	2	2	8	4	16
KR-12-a5(6-^{D}L)	2	8	2	2	4	8	16
KR-12-a5(7-^{D}L)	2	4	2	2	8	4	16
LL-37	4	8	4	4	16	8	16

Control represents bacteria treated with peptide only.

조선대학교
CHOSUN UNIVERSITY

Table 8. FICI[a] for the peptides in combination with conventional antibiotics against MDRPA (CCARM 2095).

Peptide	Chloramphenicol	Ciprofloxacin	Oxacillin
KR-12-a5	0.25 (64/512 + 2/16)	0.3125 (128/512 + 1/16)	0.375 (256/1024 + 2/16)
KR-12-a5(5-^{D}K)	0.375 (64/512 + 2/8)	0.50 (128/512 + 2/8)	0.375 (128/1024 + 2/8)
KR-12-a5(6-^{D}L)	0.375 (128/512 + 1/8)	0.3125 (128/512 + 0.5/8)	0.50 (256/1024 + 2/8)
KR-12-a5(7-^{D}L)	0.50 (128/512 + 2/8)	0.3125 (128/512 + 0.5/8)	0.3125 (256/1024 + 0.5/8)
LL-37	0.75 (256/512 + 2/8)	1.0 (256/512 + 4/8)	1.50 (1024/1024 + 4/8)

[a] FICI = (MIC of antibiotic in combination) / (MIC of antibiotic alone) + (MIC of peptide in combination) / (MIC of peptide alone).

FICI < 0.5 is synergy, 0.5 < FICI < 1.0 is additive, 1.0< FICI < 4.0 is indifferent, and FICI > 4.0 is antagonism.

조선대학교
CHOSUN UNIVERSITY

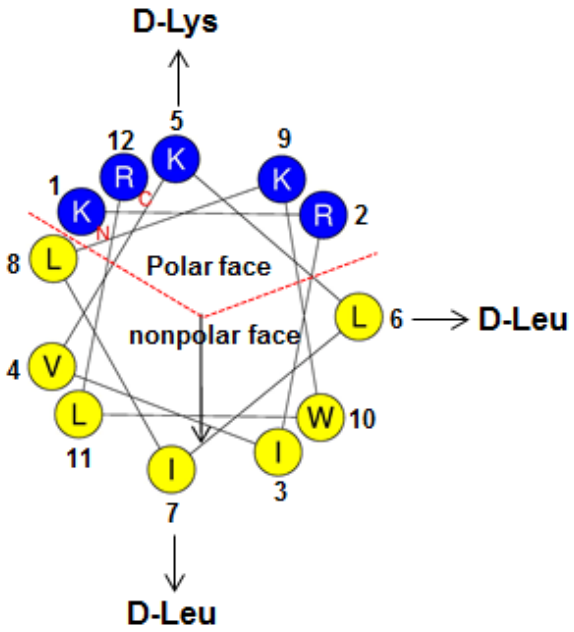

Fig. 1. Helical wheel projection diagrams of KR-12-a5 and its analogs. Positively charged residues are represented using blue circles, and hydrophobic (nonpolar) residues using yellow circles.

조선대학교
CHOSUN UNIVERSITY

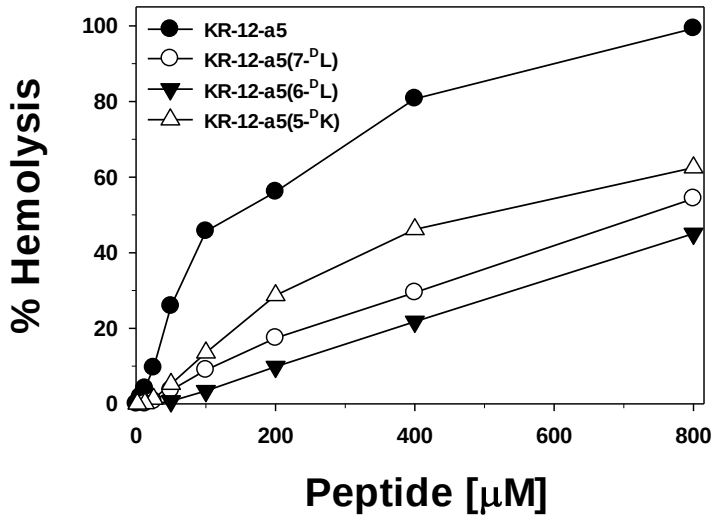

Fig. 2. Dose-response curves for human red blood cell hemolysis induced by KR-12-a5 and its analogs

조선대학교
CHOSUN UNIVERSITY

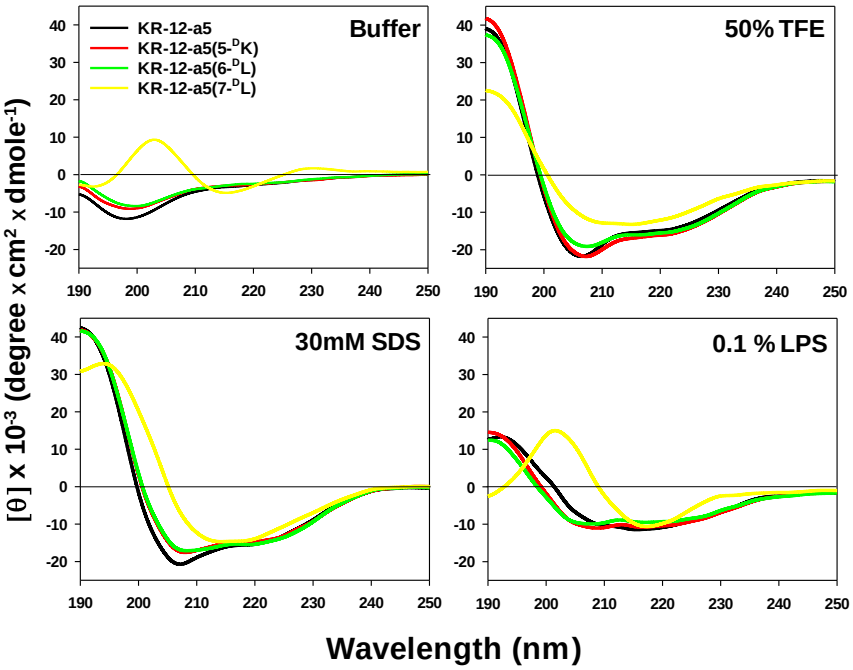

Fig. 3. The CD spectra of KR-12-a5 and its analogs. The peptides were dissolved in 10 mM sodium phosphate buffer (pH 7.4), 50% TFE, 30 mM SDS or 0.1% LPS. The mean residue ellipticity was plotted against wavelength. The values from three scans were averaged per sample.

조선대학교
CHOSUN UNIVERSITY

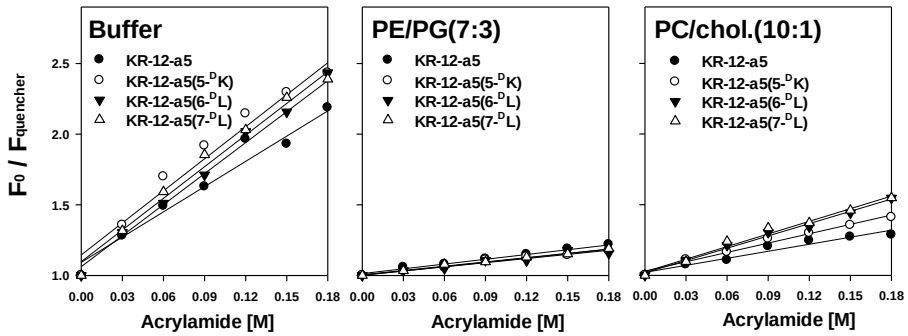

Fig. 4. Stern-Volmer plots for the quenching of Trp fluorescence of the peptides by an aqueous quencher, acrylamide, in Tris–HCl buffer (pH 7.2) alone, or in the presence of PE/PG (7:3, w/w) SUVs, or PC/cholesterol (10:1, w/w) SUVs.

조선대학교
CHOSUN UNIVERSITY

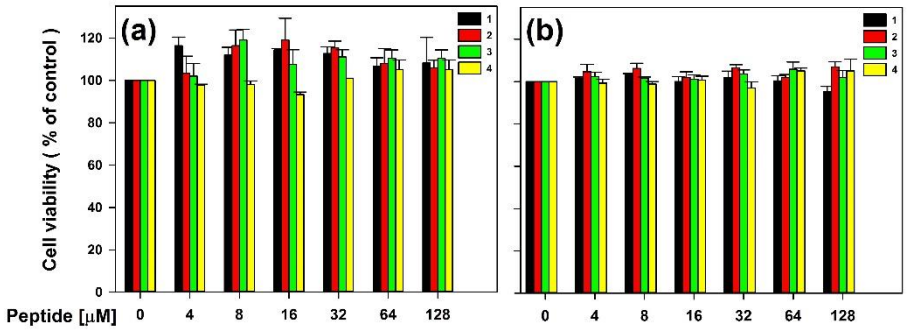

Fig. 5. Cytotoxicity of KR-12-a5 and its analogs against mouse macrophage RAW264.7 cells (a) and mouse NIH-3T3 fibroblast cells (b). 1: KR-12-a5, 2: KR-12-a5(5-^{D}K), 3: KR-12-a5(6-^{D}L), 4: KR-12-a5(7-^{D}L).

조선대학교
CHOSUN UNIVERSITY

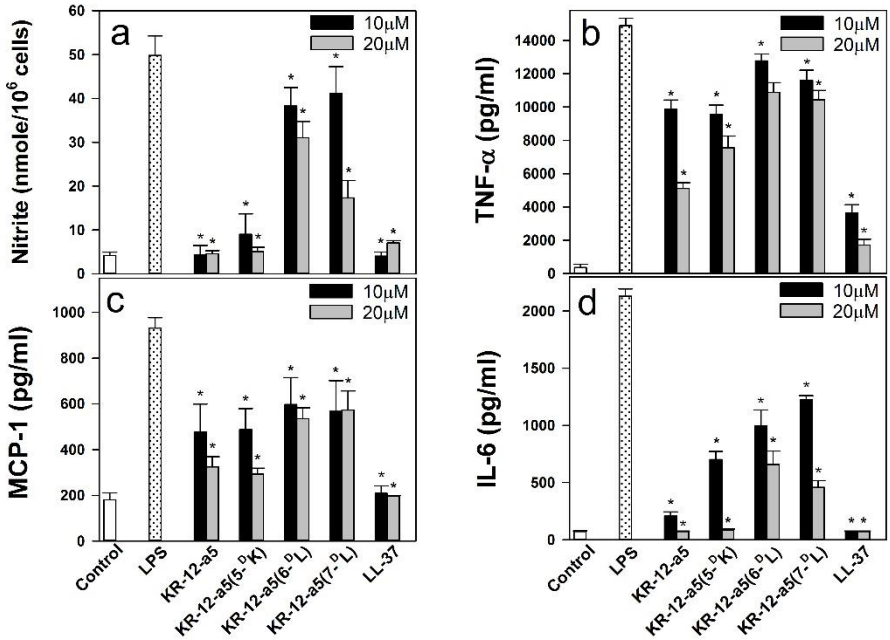

Fig. 6. Effects of the peptides on the release of NO, TNF-α, IL-6 and MCP-1 from LPS-stimulated RAW264.7 cells. RAW264.7 cells were stimulated with LPS (20 ng/ml) in the presence and absence (control) of peptides (10 and 20 μM). Secreted NO, TNF-α, IL-6 and MCP-1 were measured from the supernatants after 24 hr of LPS-stimulation by ELISA. Asterisks indicate significant effects of peptides compared to LPS treated cells. Data were analyzed by one-way analysis of variance (ANOVA) with Bonferroni's post-test ($^{*}p < 0.001$ for each agonist). The data are mean ± SEM of technical triplicates, and the findings were similar when the experiments were repeated using different cells.

조선대학교
CHOSUN UNIVERSITY

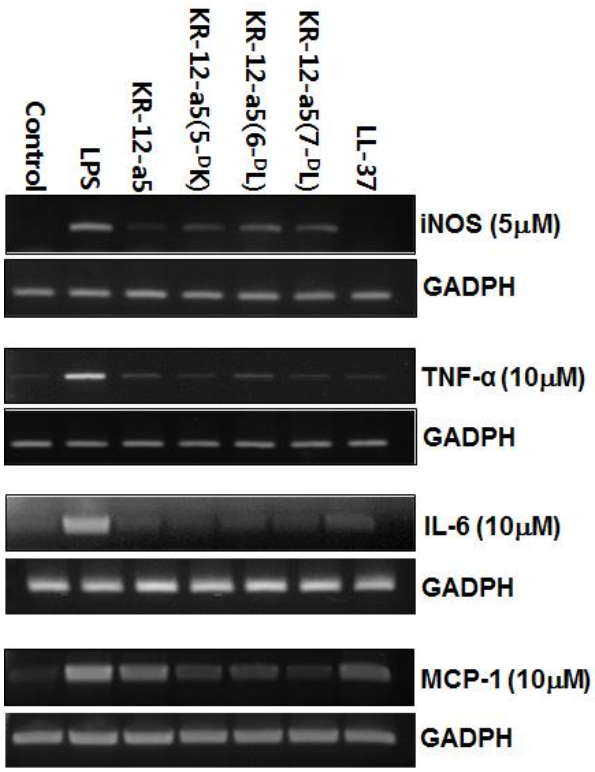

Fig. 7. Effects of KR-12-a5, its analogs and LL-37 on the mRNA expression of iNOS, TNF-α, IL-6 and MCP-1 in LPS-stimulated RAW264.7 cells. RAW264.7 cells (5×10^5 cells/well) were incubated with the peptides in the presence of LPS (20 ng/ml) for 3 h (for TNF-α, IL-6, and MCP-1) or 6 h (for iNOS). Total RNA was isolated and analyzed to determine the levels of mRNAs of iNOS, TNF-α, IL-6 and MCP-1 by RT-PCR.

조선대학교
CHOSUN UNIVERSITY

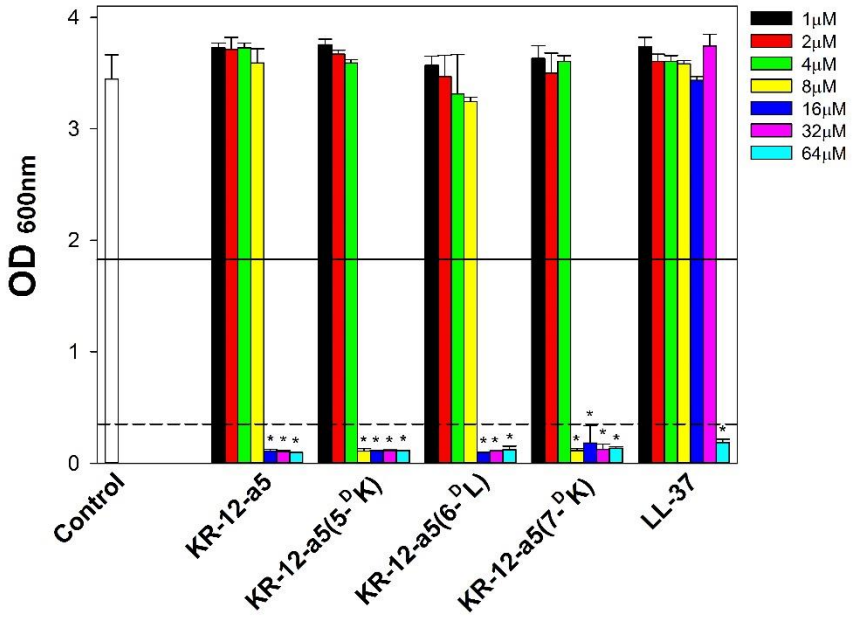

Fig. 8. Inhibitory effect of KR-12-a5, its analogs and LL-37 on MDRPA biofilm formation. MDRPA (CCARM 2095) was incubated for 24 h with the indicated concentrations of peptides. After the incubation, crystal violet was used to stain the biofilm. The stain was dissolved in 95% ethanol and absorbance at 600 nm (OD_{600}) was measured. Values are means ± SEM of technical triplicates. Solid lines and dotted lines represent 50% and 90% reduction in biofilm biomass, respectively, relative to that of control biofilms. Data were analyzed using one-way analysis of variance (ANOVA) with Bonferroni's post-test. An asterisk indicates a significant effect ($^{*}p < 0.001$ for each agonist) of the peptide compared to that of control (i.e., absence of peptide). Results were similar when the experiments were repeated with different cells.

조선대학교
CHOSUN UNIVERSITY

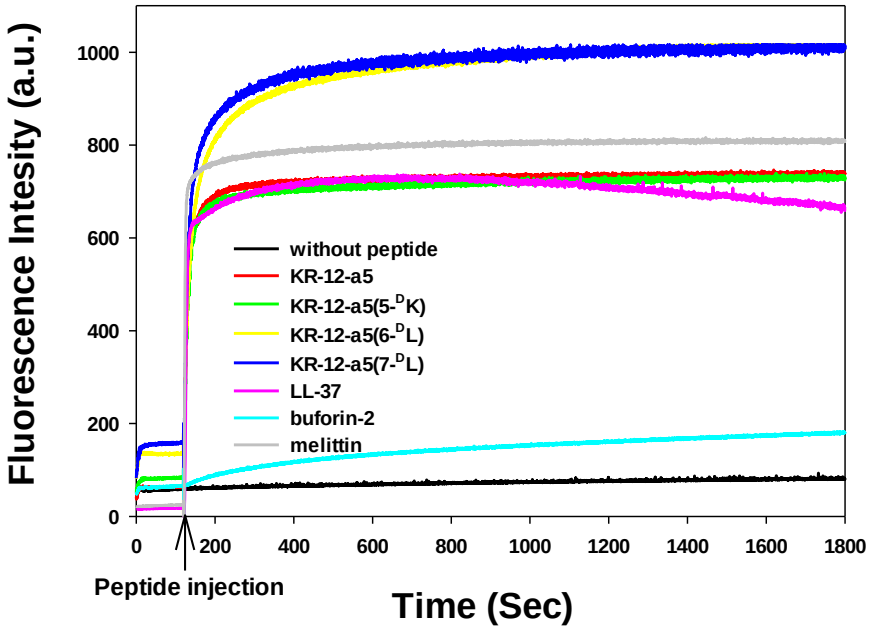

Fig. 9. Kinetics of *S. aureus* membrane permeabilization caused by KR-12-a5 and its analogs at 2 × MIC. The positive control peptides (LL-37 and melittin) and negative control peptide (buforin-2) are also shown. Alterations of the cytoplasmic membrane allow the SYTOX Green probe to enter the cell and bind DNA, resulting in an increase of fluorescence.

조선대학교
CHOSUN UNIVERSITY

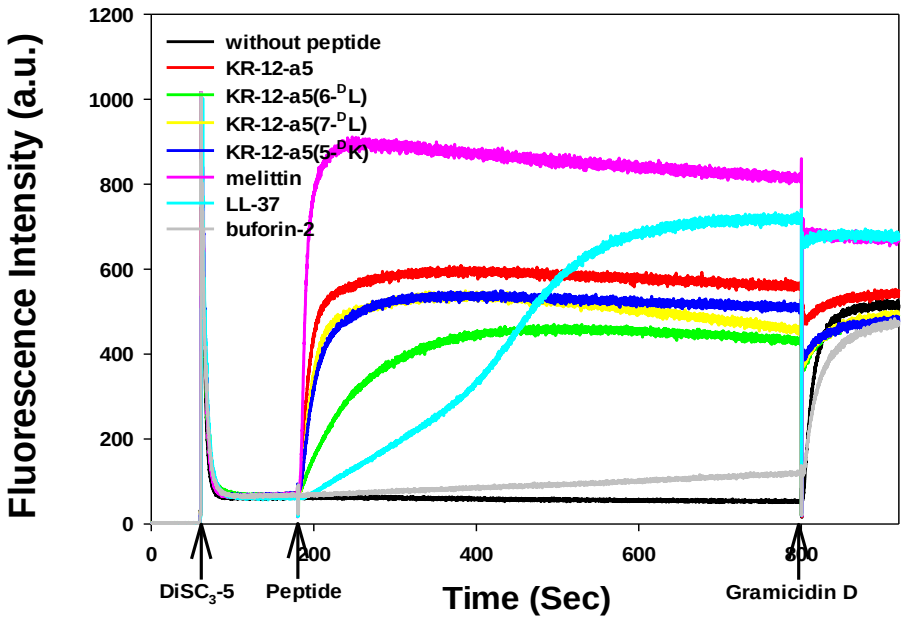

Fig. 10. The depolarization of *S. aureus* cytoplasmic membrane induced by KR-12-a5 and its analogs at 2 × MIC, determined using the membrane potential-sensitive fluorescent dye diSC$_3$-5. Dye release was monitored by measuring fluorescence, at an excitation wavelength of 622 nm and an emission wavelength of 670 nm, and plotting the emission against time. Curves corresponding to the positive control peptides (LL-37 and melittin) and negative control peptide (buforin-2) are also shown.

조선대학교
CHOSUN UNIVERSITY

References

[1] B. Mishra, S. Reiling, D. Zarena, G. Wang, Host defense antimicrobial peptides as antibiotics: design and application strategies, Curr. Opin. Chem. Biol. 38 (2017) 87–96.

[2] D.I. Andersson, D. Hughes, J.Z. Kubicek-Sutherland, Mechanisms and consequences of bacterial resistance to antimicrobial peptides. Drug Resist. Updat. 26 (2016) 43–57.

[3] S. Ramesh, T. Govender, H.G. Kruger, B.G. de la Torre, F. Albericio, Short antimicrobial peptides (SAMPs) as a class of extraordinary promising therapeutic agents, J. Pept. Sci. 22 (2016) 438–451.

[4] N.J. Afacan, A.T. Yeung, O.M. Pena, R.E. Hancock, Therapeutic potential of host defense peptides in antibiotic-resistant infections, Curr. Pharm. Des. 18 (2012) 807–819.

[5] E.F. Haney, S.C. Mansour, R.E. Hancock, Antimicrobial Peptides: An Introduction, Methods Mol. Biol. 1548 (2017) 3–22.

[6] G.H. Gudmundsson, B. Agerberth, J. Odeberg, T. Bergman, B. Olsson, R. Salcedo, The human gene FALL39 and processing of the cathelin precursor to the antibacterial peptide LL-37 in granulocytes, Eur. J. Biochem. 238 (1996) 325–332.

[7] O.E. Sørensen, P. Follin, A.H. Johnsen, J. Calafat, G.S. Tjabringa, P.S. Hiemstra, N. Borregaard, Human cathelicidin, hCAP-18, is processed to the antimicrobial peptide LL-37 by extracellular cleavage with proteinase 3, Blood 97 (2001) 3951–3959.

[8] J. Turner, Y. Cho, N.N. Dinh, A.J. Waring, R.I. Lehrer, Activities of LL-37, a cathelin-associated antimicrobial peptide of human neutrophils, Antimicrob.

조선대학교
CHOSUN UNIVERSITY

Agents Chemother. 42 (1998) 2206–2214.

[9] J.E. Gable, D.E. Schlamadinger, A.L. Cogen, R.L. Gallo, J.E. Kim, Fluorescence and UV resonance Raman study of peptide-vesicle interactions of human cathelicidin LL-37 and its F6W and F17W mutants, Biochemistry 48 (2009) 11264–11272.

[10] K.A. Henzler Wildmanm, D.K. Lee, A. Ramamoorthy, Mechanism of lipid bilayer disruption by the human antimicrobial peptide, LL-37, Biochemistry 42 (2003) 6545–6558.

[11] C.C. Lee, Y. Sun, S. Qian, H.W. Huang, Transmembrane pores formed by human antimicrobial peptide LL-37, Biophys. J. 100 (2011) 1688–1696.

[12] S.M. Alalwani, J. Sierigk, C. Herr, O. Pinkenburg, R. Gallo, C. Vogelmeier, R. Bals, The antimicrobial peptide LL-37 modulates the inflammatory and host defense response of human neutrophils, Eur. J. Immunol. 40 (2010) 1118–1126.

[13] S.H. Lee, H.K. Jun, H.R. Lee, C.P. Chung, B.K. Choi, Antibacterial and lipopolysaccharide (LPS)-neutralising activity of human cationic antimicrobial peptides against periodontopathogens, Int. J. Antimicrob. Agents 35 (2010) 138–145.

[14] M. Golec, Cathelicidin LL-37: LPS-neutralizing, pleiotropic peptide, Ann. Agric. Environ. Med. 14 (2007) 1–4.

[15] T. Into, M. Inomata, K. Shibata, Y. Murakami, Effect of the antimicrobial peptide LL-37 on Toll-like receptors 2-, 3- and 4- triggered expression of IL-6, IL-8 and CXCL10 in human gingival fibroblasts, Cell. Immunol. 264 (2010) 104–109.

조선대학교
CHOSUN UNIVERSITY

[16] X. Li, Y. Li, H. Han, D.W. Miller, G. Wang, Solution structures of human LL-37 fragments and NMR-based identification of a minimal membrane-targeting antimicrobial and anticancer region, J. Am. Chem. Soc. 128 (2006) 5776–5785.

[17] G. Wang, Structures of human host defense cathelicidin LL-37 and its smallest antimicrobial peptide KR-12 in lipid micelles, J. Biol. Chem. 283 (2008) 32637–32643.

[18] Y.H. Nan, J.K. Bang, B. Jacob, I.S. Park, S.Y. Shin, Prokaryotic selectivity and LPS-neutralizing activity of short antimicrobial peptides designed from the human antimicrobial peptide LL-37, Peptides 35 (2012) 239–247.

[19] B. Jacob, I.S. Park, J.K. Bang, S.Y. Shin, Short KR-12 analogs designed from human cathelicidin LL-37 possessing both antimicrobial and antiendotoxic activities without mammalian cell toxicity, J. Pept. Sci. 19 (2013) 700–707.

[20] K.Y. Choi, S. Napper, N. Mookherjee, Human cathelicidin LL-37 and its derivative IG-19 regulate interleukin-32-induced inflammation, Immunology 143 (2014) 68–80.

[21] L.R. McLean, K.A. Hagaman, T.J. Owen, J.L. Krstenansky, Minimal peptide length for interaction of amphipathic α-helical peptides with phosphatidylcholine liposomes, Biochemistry 30 (1991) 31–37.

[22] A.I. De Kroon, M.W. Soekarjo, J. De Gier, B. De Kruijff, The role of charge and hydrophobicity in peptide–lipid interaction: a comparative study based on tryptophan fluorescence measurements combined with the use of aqueous and hydrophobic quenchers, Biochemistry 29 (1990) 8229–8240.

[23] W.L. Zhu, H. Lan, I.S. Park, J.L. Kim, H.Z. Jin, K.S. Hahm, S.Y. Shin, Design and mechanism of action of a novel bacteria selective antimicrobial peptide from the cell-penetrating peptide Pep-1, Biochem. Biophys. Res. Commun. 349

조선대학교
CHOSUN UNIVERSITY

(2006) 769–774.

[24] G. Rajasekaran, E.Y. Kim, S.Y. Shin. LL-37-derived membrane-active FK-13 analogs possessing cell selectivity, anti-biofilm activity and synergy with chloramphenicol and anti-inflammatory activity, Biochim. Biophys. Acta 1859 (2017) 722-733.

[25] G. Batoni, M. Casu, A. Giuliani, V. Luca, G. Maisetta, M.L. Mangoni, G. Manzo, M. Pintus, G. Pirri, A.C. Rinaldi, M.A. Scorciapino, I. Serra, A.S. Ulrich, P. Wadhwani, Rational modification of a dendrimeric peptide with antimicrobial activity: consequences on membrane-binding and biological properties, Amino Acids 48 (2016) 887–900.

[26] K. Rand, H. Houck, P. Brown, D. Bennett, Reproducibility of the microdilution checkerboard method for antibiotic synergy, Antimicrob. Agents Chemother. 37 (1993) 613–615.

[27] P.J. Petersen, P. Labthavikul, C.H. Jones, P.A. Bradford, In vitro antibacterial activities of tigecycline in combination with other antimicrobial agents determined by chequerboard and time-kill kinetic analysis, J. Antimicrob. Chemother. 57 (2006) 573–576.

[28] J.S. Khara, Y. Wang, X.Y. Ke, S. Liu, S.M. Newton, P.R. Langford, Y.Y. Yang, P.L. Ee, Antimycobacterial activities of synthetic cationic α-helical peptides and their synergism with rifampicin, Biomaterials 35 (2014) 2032–2038.

[29] M. Wu, R.E. Hancock, Interaction of the cyclic antimicrobial cationic peptide bactenecin with the outer and cytoplasmic membrane, J. Biol. Chem. 274 (1999) 29–35.

[30] C.L. Friedrich, A. Rozek, A. Patrzykat, R.E. Hancock, Structure and

조선대학교
CHOSUN UNIVERSITY

mechanism of action of an indolicidin peptide derivative with improved activity against gram-positive bacteria, J. Biol. Chem. 276 (2001) 24015–24022.

[31] B.L. Roth, M. Poot, S.T. Yue, P.J. Millard, Bacterial viability and antibiotic susceptibility testing with SYTOX green nucleic acid stain, Appl. Environ. Microbiol. 63 (1997) 2421–2431.

[32] S. Kim, S.S. Kim, B.J. Lee, Correlation between the activities of α-helical antimicrobial peptides and hydrophobicities represented as RP-HPLC retention times, Peptides 26 (2005) 2050–2056.

[33] X. Dou, X. Zhu, J. Wang, N. Dong, A. Shan, Novel design of heptad amphiphiles to enhance cell selectivity, salt resistance, anti-biofilm properties and their membrane-disruptive mechanism, J. Med. Chem. 60 (2017) 2257–2270.

[34] N. Dong, X. Zhu, S. Chou, A. Shan, W. Li, J. Jiang, Antimicrobial potency and selectivity of simplified symmetric-end peptides, Biomaterials 35 (2014) 8028–8039.

[35] R.M. Dawson, M.A. Fox, H.S. Atkins, C.Q. Liu, Potent antimicrobial peptides with selectivity for *Bacillus anthracis* over human erythrocytes, Int. J. Antimicrob. Agents 38 (2011) 237– 242.

[36] S. Rex, Pore formation induced by the peptide melittin in different lipid vesicle membranes, Biophys. Chem. 58 (1996) 75－85.

[37] C.B. Park, H.S. Kim, S.C. Kim, Mechanism of action of the antimicrobial peptide buforin II: Buforin II kills microorganisms by penetrating the cell membrane and inhibiting cellular functions, Biochem. Biophys. Res. Comm. 244 (1998) 253–257.

[38] Y. Shai, Z. Oren, Diastereoisomers of cytolysins, a novel class of potent

조선대학교
CHOSUN UNIVERSITY

antibacterial peptides, J Biol. Chem. 271 (1996) 7305–7308.

[39] Z. Oren, Y. Shai, Selective lysis of bacteria but not mammalian cells by diastereomers of melittin: structure-function study, Biochemistry 36 (1997) 1826–1835.

[40] Z. Oren, J. Hong, Y. Shai, A repertoire of novel antibacterial diastereomeric peptides with selective cytolytic activity, J. Biol. Chem. 272 (1997) 14643–14649.

[41] M.E. Evans, M. Pollack, Effect of antibiotic class and concentration on the release of

lipopolysaccharide from *Escherichia coli*, J. Infect. Dis. 167 (1993) 1336–1343.

[42] M.S. Trent, M.C. Stead, A.X. Tran, J.V. Hankins, Diversity of endotoxin and its impact on pathogenesis, J. Endotoxin Res. 12 (2006) 205–223.

[43] Y. Rosenfeld, N. Papo, Y. Shai, Endotoxin (lipopolysaccharide) Neutralization by innate immunity host-defense peptides, J. Biol. Chem. 281 (2006) 1636–1643.

[44] N. Papo. Y.A. Shai, Molecular mechanism for lipopolysaccharide protection of Gram-negative bacteria from antimicrobial peptides, J. Biol. Chem. 280 (2005) 10378–10387.

[45] G.S. Martin, D.M. Mannino, S. Eaton, M. Moss, The epidemiology of sepsis in the United States from 1979 through 2000, N. Engl. J. Med. 348 (2003) 1546–1554.

[46] J.W. Larrick, M. Hirata, R.F. Balint, J. Lee, J. Zhong, S.C. Wright, Human CAP18: a novel antimicrobial lipopolysaccharide-binding protein, Infect. Immun. 63 (1995) 1291–1297.

조선대학교
CHOSUN UNIVERSITY

[47] C.D. Ciornei, T. Sigurdardóttir, A. Schmidtchen, M. Bodelsson, Antimicrobial and chemoattractant activity, lipopolysaccharide neutralization, cytotoxicity, and inhibition by serum of analogs of human cathelicidin LL-37, Antimicrob. Agents Chemother. 49 (2005) 2845–2850.

[48] T. Sawa, K. Kurahashi, M. Ohara, M. Gropper, V. Doshi, J.W. Larrick, J.P. Wiener-Kronish, Evaluation of antimicrobial and lipopolysaccharide-neutralizing effects of a synthetic CAP18 fragment against Pseudomonas aeruginosa in a mouse model, Antimicrob. Agents Chemother. 42 (1998) 3269–3275.

[49] I. Nagaoka, S. Hirota, F. Niyonsaba, M. Hirata, Y. Adachi, H. Tamura, D. Heumann, Cathelicidin family of antibacterial peptides CAP18 and CAP11 inhibit the expression of TNF-α by blocking the binding of LPS to $CD14^{+}$ cells, J. Immunol. 167 (2001) 3329–3338.

[50] F. Torres-Juarez, A. Cardenas-Vargas, A. Montoya-Rosales, I. González-Curiel, M.H. Garcia-Hernandez, J.A. Enciso-Moreno, R.E. Hancock, B. Rivas-Santiago, LL-37 immunomodulatory activity during Mycobacterium tuberculosis infection in macrophages, Infect. Immun. 83 (2015) 4495–4503.

[51] H.L. Chu, H.Y. Yu, B.S. Yip, Y.H. Chih, C.W. Liang, H.T. Cheng, J.W. Cheng, Boosting salt resistance of short antimicrobial peptides, Antimicrob. Agents Chemother. 57 (2013) 4050–4052.

[52] J. Huang, D. Hao, Y. Chen, Y. Xu, J. Tan, Y. Huang, F. Li, Y. Chen, Inhibitory effects and mechanisms of physiological conditions on the activity of enantiomeric forms of an α-helical antibacterial peptide against bacteria, Peptides 32 (2011) 1488–1495.

[53] P. Gilbert, D. Allison, A. McBain, Biofilms in vitro and in vivo: do singular

조선대학교
CHOSUN UNIVERSITY

mechanisms imply cross-resistance? J. Appl. Microbiol. 92 (2002) 98S–110S.

[54] J.B. Lyczak, C.L. Cannon, G.B. Pier, Lung infections associated with cystic fibrosis, Clin. Microbiol. Rev. 15 (2002) 194–222.

[55] J. Overhage, A. Campisano, M. Bains, E.C. Torfs, B.H. Rehm, R.E. Hancock, Human host defense peptide LL-37 prevents bacterial biofilm formation, Infect. Immun. 76 (2008) 4176–4182.

[56] A. Pompilio, M. Scocchi, S. Pomponio, F. Guida, A. Di Primio, E. Fiscarelli, R. Gennaro, G. Di Bonaventura, Antibacterial and anti-biofilm effects of cathelicidin peptides against pathogens isolated from cystic fibrosis patients, Peptides 32 (2011) 1807–1814.

[57] T. Tangden, Combination antibiotic therapy for multidrug-resistant Gram-negative bacteria, Ups. J. Med. Sci. 119 (2014) 149–153.

[58] A.I. Zumla, S.H. Gillespie, M. Hoelscher, P.P. Philips, S.T. Cole, I. Abubakar, T.D. McHugh, M. Schito, M. Maeurer, A.J. Nunn, New antituberculosis drugs, regimens, and adjunct therapies: needs, advances, and future prospects, Lancet Infect. Dis. 14 (2014) 327–340.

[59] A. Giacometti, O. Cirioni, M.S. Del Prete, F. Barchiesi, M. Fortuna, D. Drenaggi, G. Scalise, In vitro activities of membrane-active peptides alone and in combination with clinically used antimicrobial agents against *Stenotrophomonas maltophilia*, Antimicrob Agents Chemother. 44 (2000) 1716–1719.

[60] L. Fassi Fehri, H. Wróblewski, A. Blanchard, Activities of antimicrobial peptides and synergy with enrofloxacin against *Mycoplasma pulmonis*, Antimicrob. Agents Chemother. 51 (2007) 468–474.

[61] Z. Oren, Y. Shai, Mode of action of linear amphipathic α-helical antimicrobial

조선대학교
CHOSUN UNIVERSITY

peptides, Biopolymers 47 (1998) 451–463.

[62] O. Toke, Antimicrobial peptides: new candidates in the fight against bacterial infections, Biopolymers 80 (2005) 717–735.

조선대학교
CHOSUN UNIVERSITY

PART II

Mechanisms of Antimicrobial and Anti-Endotoxin Activities of a Triazine-Based Amphipathic Polymer

조선대학교
CHOSUN UNIVERSITY

1. Introduction

Although conventional antimicrobials are widely used to treat bacterial infections in clinical applications, antimicrobial resistance (AMR) and the emergence of multidrug-resistant bacterial strains, due to the overuse and abuse of antimicrobials, is a serious threat to public health worldwide (Giamarellou, 2006; Walsh, & Wencewicz, 2014). Thus, to overcome AMR, antimicrobials with new mechanisms of action are urgently needed (Blair, Webber, Baylay, Ogbolu, & Piddock, 2015). Antimicrobial peptides (AMPs) are essential components of innate immunity in most living organisms. AMPs are promising antimicrobial candidates with the potential to overcome bacterial drug resistance due to their membrane-active properties, rapid killing ability, and broad-spectrum activities (Marín-Medina, Ramírez, Trier, & Leidy, 2016). Although AMPs have advantages over conventional antimicrobials, their clinical application has been limited by several factors, such as poor stability upon proteolysis, moderate activity, and high manufacturing costs. To circumvent these drawbacks, synthetic small-molecule peptidomimetics that mimic the structure and function of AMPs have been employed recently as an alternative approach, with the aim of achieving similar antimicrobial activity, but with improved pharmacokinetic properties (Ahn et al., 2017; Ghosh, & Haldar, 2015; Gunasekaran, et al., 2019).

Recently, our group designed a new series of small-molecule triazine-based amphipathic polymers (TZPs) that mimic the amphipathic structures found in AMPs (Gunasekaran, et al., 2019). Of the designed TZPs, TZP3, TZP4, TZP5, TZP6, and TZP9 showed potent antimicrobial activity against gram-positive and gram-negative bacterial pathogens with minimum inhibitory concentrations (MICs) ranging from 2 to 8 μg/mL and no hemolytic activity even at 256 μg/mL,

조선대학교
CHOSUN UNIVERSITY

which was the highest concentration tested. In particular, TZP3 and TZP5 had a significant anti-atopic effect on atopic-like skin lesions in a BALB/c mouse model (Gunasekaran, et al., 2019). TZP3 and TZP5 significantly inhibited the release of β-hexosaminidase and tumor necrosis factor-α (TNF-α) from RBL-2H3 cells (rat basophilic leukemia cell line). In addition, these two polymers displayed remarkable inhibitory effects on TNF-α, TGF-β, iNOS, and COX-2 protein levels in RBL-2H3 rat tumor mast cells (Gunasekaran, et al., 2019). Thus, TZP3 and TZP5 may be new models for the design of antimicrobial agents with anti-atopic activity, but without mammalian cell toxicity.

The therapeutic potential of antimicrobial agents depends on their ability to selectively kill bacteria and not normal mammalian cells. The therapeutic index (TI) is used to evaluate the cell selectivity of antimicrobial agents towards negatively charged bacterial cell membranes over zwitterionic mammalian cell membranes. TZP4 and TZP6 show excellent antimicrobial activity against the tested bacterial strains, with low toxicity and thus, have the highest cell selectivity (TI ≈205). Although TZP4 and TZP6 were found to show similar antimicrobial potential and TI, the molecular weight of TZP-4 (MW: 857.5) is relatively low compared to TZP6 (M.W: 941.5). Moreover, the synthesis of guanidine anchored hydrophilic triazine monomers requires one step more compared to the amine anchored hydrophilic triazine monomers. Thus, to investigate bactericidal mechanism of TZPs and inhibitory activity against LPS-induced inflammation in macrophages, TZP4 **(**Figure 1**)** was chosen as the better polymer. The antimicrobial action of TZP4 were investigated by cytoplasmic membrane depolarization, SYTOX Green uptake, flow cytometry, and gel retardation assays. Afterward, the proteolytic resistance of TZP4 to digestive enzymes such as pepsin, trypsin and α-chymotrypsin

조선대학교
CHOSUN UNIVERSITY

investigated. Furthermore, the development of antibiotic resistance in *S. aureus* for TZP4 after serial passages were investigated.

Recently, it has been emphasized that effective antimicrobial agents should have both direct bactericidal activity and significant inhibitory activity against the inflammatory responses induced by the major component of the outer membrane of gram-negative bacteria, LPS, which is also known as an endotoxin. Thus, to assess the potential of TZP4 as an anti-endotoxin drug against LPS-induced inflammation, we measured the effect of TZP4 on nitric oxide (NO) and TNF-α production and mRNA expressions of *iNOS* and *TNF-α* in LPS-stimulated RAW 264.7 mouse cells. Furthermore, TZP4 was investigated for its ability to bind and dissociate the LPS oligomers, and its ability to inhibit the interaction of LPS to the CD14 receptor of macrophages.

조선대학교
CHOSUN UNIVERSITY

2. Materials and Methods

2.1 Materials

Lipopolysaccharide (LPS) purified from *Escherichia col*i O111:B4, (3-[4,5 dimethylthiozol-2-yl]-2,5-diphenyltetrazolium bromide) (MTT), $DiSC_3$-5, pepsin (EC 3.4.23.1, Sigma), trypsin (EC 3.4.21.4, Sigma), and α-chymotrypsin (EC 3.4.21.1, Sigma) were supplied from Sigma-Aldrich (St. Louis, MO, USA). HyClone Dulbecco's modified Eagle medium (DMEM) and fetal bovine serum (FBS) were obtained from SeouLin Bioscience (Seoul, Korea). The ELISA kits for TNF-*α* was procured from R&D Systems (Minneapolis, MN, USA). SYTOX green was purchased from Life Technologies (Eugene, OR, USA). *Escherichia coli* (KCTC 1682) and *Staphylococcus aureu*s (KCTC 1621) and were procured from the Korean Collection for Type Cultures (KCTC) of the Korea Research Institute of Bioscience and Biotechnology (KRIBB). Methicillin-resistant *Staphylococcus aureu*s strains (MRSA; CCARM 3089, and CCARM 3090) and multidrug-resistant Pseudomonas aeruginosa strains (MDRPA; CCARM 2095, and CCARM 2109) were obtained from the Culture Collection of Antibiotic-Resistant Microbes (CCARM) of Seoul Women's University in Korea.

2.2 Antimicrobial activity

The minimal inhibitory (MICs) of TZP4, melittin and conventional concentrations antibiotics against aforementioned antibiotic-resistant bacterial strains were determined by the modified broth microdilution method of the National Committee for Clinical Laboratory Standards (NCCLS), as previously described (Chou et al., 2016; Wang et al., 2018). In brief, mid-logarithmic phase of MRSA

조선대학교
CHOSUN UNIVERSITY

(CCARM 3089 and CCARM 3090) and MDRPA (CCARM 2095 and CCARM 2109) were diluted with Mueller-Hinton broth (MHB) (Difco, USA), and added to a microtiter plate (2×10^6 CFU/well). A two-fold serial dilution of samples was subsequently added, and the plate was incubated for 24 hours at 37 ℃. The experiment was performed in triplicate using three replicates for each sample and each bacterium. The lowest peptide concentration which gave no visible growth is determined as the MIC value.

2.3 Time-killing kinetics assay

Bactericidal kinetics of TZP4 was determined as described previously (Koh et al., 2013). Briefly, mid-logarithmic phase *E. coli* (KCTC 1682) and *S. aureus* (KCTC 1621) were adjusted to 1×10^6 CFU/mL in MHB media and treated with TZP4 and melittin at their respective MICs for 0, 1, 2, 5, 10, 20, 40 and 60 mins at 37 ℃. At each time of exposure, 50 μL aliquots of mixture was diluted with fresh MHB media for tenfold (up to 1000 times), then 100 μL of diluted bacterial suspension was plated onto MH agar plates to obtain viability counts. Colonies were counted after incubation for 24 h at 37 ℃.

2.4 Protease stability by radial diffusion assay

Escherichia coli (KCTC 1682) was grown overnight to stationary phase at 37 ℃ in 10 mL of Luria-Bertani (LB) medium (Difco, USA). The overnight cultures were 10-fold diluted in fresh LB broth and incubated for additional 3h at 37 ℃ to obtain mid-log phase organisms. A bacteria suspension (2×10^6 CFU/mL in LB) was mixed with 0.7% agarose and poured into a 10 cm petri dish, and dispersed rapidly. Five microliters of an aqueous TZP4 stock solution (10 mg/mL) were

조선대학교
CHOSUN UNIVERSITY

added to 25 μL of pepsin (pH 2.0), trypsin (pH 7.4), and α-chymotrypsin (pH 7.4) stock solution (0.2 mg/mL) in 50 mM Tris-HCl buffer, and incubated at 37 ℃ for 4 h. The reaction was stopped by freezing with liquid nitrogen, after which 30 μL of aliquots were added to each circle paper (6 mm in diameter) placed on the agarose plates, and then incubated at 37 ℃ overnight. The diameters of the bacterial clearance zones surrounding the circle paper were measured for the quantitation of inhibitory activities.

2.5 Drug resistance assay

To explore the acquired resistance tendency of *S. aureus* (KCTC 1621) to TZP4 and ciprofloxacin, the drug resistance assay was assessed by sequential passages as previously described (Pollard et al., 2012; Lyu et al., 2017). MIC testing was firstly conducted for the peptides using the above methods. Then, the 0.5 × MIC well from the previous MIC assay plate was re-suspended and the bacteria was cultured in fresh MHB medium. The inoculum was subjected to the next passage MIC testing, and the process was repeated for 15 passages.

2.6 Cytoplasmic membrane depolarization assay

The cytoplasmic membrane electrical potential change induced by TZP4 was determined with the membrane potential-sensitive fluorescent dye, $DiSC_3$-5 (Sigma-Aldrich, USA) as previously described (Chou et al., 2016; Lyu, Yang, Lyu, Dong, & Shan, 2016; Zhu et al., 2015). Briefly, mid-log phase *S. aureus* (KCTC 1621) was harvested and washed three times with 5mM HEPES buffer (pH 7.4, containing 20 mM glucose). The cells were then resuspended to

조선대학교
CHOSUN UNIVERSITY

$A_{600nm}=0.05$ in same buffer containing 100 mM KCl, after which 0.4 μM $DiSC_3$-5 was added and background fluorescence was recorded (excitation λ = 622 nm, emission λ = 670 nm) until a stable fluorescence reduction was achieved, implying the complete incorporation of the dye into the bacterial membrane. Subsequently, 2× MIC of TZP4 and peptides (melittin and buforin-2) was then added to bacterial suspension and changes in fluorescence intensity was recorded using a RF-5301 PC Spectrofluorophotometer (Shimadzu, Japan).

2.7 SYTOX green uptake assay

Mid-logarithmic phase of *S. aureus* (KCTC 1621) cells were washed and resuspended to an A_{600nm} = 0.08 in HEPES buffer (pH 7.4, containing 20 mM glucose and 100mM KCL). SYTOX Green (Thermo Fisher Scientific, USA) was added to a final concentration of 1 mM, and the cells were incubated at 37 °C for 15 min with agitation in dark. Thereafter, 2× MIC of TZP4 and peptides (melittin, LL-37 and buforin-2) was added and the release of SYTOX Green was detected (excitation λ = 485 nm, emission λ =520nm) by increase in fluorescence.

2.8 Flow cytometry analysis

The bacterial membrane integrity was determined by flow cytometry. Briefly, *E. coli* and *S. aureus* was grown to mid-log phase in LB broth, washed thrice and diluted to 2 × 10^5 CFU/mL in 1× PBS. The samples were incubated with the bacterial suspension at a fixed propidium iodide (PI) concentration of 10 μg/ml for 1 h or 2 h at 37 ℃, followed by the removal of the unbound dye through washing with an excess of PBS. The flow cytometry data were recorded using fluorescence-

조선대학교
CHOSUN UNIVERSITY

activated cell sorter (FACS Calibur, Beckman Coulter Inc., USA) at a laser excitation wavelength of 488 nm.

2.9 DNA binding assay

Gel retardation experiment was performed to evaluate the ability of compounds to bind with intracellular DNA. In brief, TZP4 or buforin-2 were mixed with a fixed concentration (100 ng) of plasmid pBR322 (Thermo Fisher Scientific, USA) from *E. coli* in a sample buffer (10 mM Tris-HCl, 5% glucose, 50 μg/mL BSA, 1 mM EDTA, and 20 mM KCl). The mixture of DNA and TZP4 or buforin-2 was incubated at 37 ˚C for 1 h and then analyzed by 1% agarose gel electrophoresis in 0.5% TAE buffer (0.8 mM Tris, 0.4 mM glacial acetic acid, 10 mM EDTA, pH 8.0). The plasmid bands were detected by UV illuminator (Bio-Rad, USA).

2.10 Cytotoxicity of TZP4 against macrophage cells

The cytotoxicity of TZP4 against mouse macrophage RAW264.7 cells was assessed by MTT assay (Dong et al., 2012). Briefly, RAW264.7 cells were cultured in DMEM (Gibco) with 10% FBS in a humidified atmosphere containing 5% CO_2 at 37 ℃. The cells were added to 96-well plates at a final concentration for 2×10^4 cells per well in DMEM and cultured overnight. TZP4 was then added and incubated for 48 hr. MTT (50 μL, 0.5 mg/mL) was added to the 96-wellplate and incubated at 37 ℃ for 4 hr. Subsequently, 150 μL of DMSO was added to dissolve the formed formazan crystals after the supernatant was discarded, and the OD was measured using a microplate reader (Bio-Tek Instruments EL800, USA) at 550 nm. Cell viability was expressed as (A_{550nm} of treated sample) / (A_{550nm} of control) 100%.

조선대학교
CHOSUN UNIVERSITY

2.11 Measurement of NO or TNF-α release from LPS-stimulated RAW264.7 cells

RAW 264.7 cells (5×10^5 cells/well) were plated in 96-well plates and stimulated with LPS from *E. coli* O111:B4 (20 ng/mL) in the absence or presence of TZP4 or LL-37 for 24 h. The culture supernatant was collected and analyzed for NO and TNF-α production using the Griess reagent (Promega) (1% sulfanilamide, 0.1% naphthylethylenediamine dihydrochloride and 2% phosphoric acid) and an enzyme-linked immunosorbent assay (R&D Systems, Minneapolis, MN, USA) according to the manufacturer's protocol, respectively. Each experiment was performed in triplicate with two biological replicates. Untreated cells and LPS only treated cells served as the respective negative and positive controls.

2.12 Reverse-transcription polymerase chain reaction (RT-PCR)

RAW264.7 cells were plated into 6-well plates at a concentration of 5×10^5 cells/well and stimulated with *E. coli* O111:B4 LPS (20 ng/mL) in the presence or absence of TZP4 or LL-37. After incubation of 3 h (for TNF-*α*) and 6 h (for inducible nitric oxide synthase (iNOS)), total RNA was extracted using TRIzol® reagent (Invitrogen) and RNA concentration quantified using Nanodrop spectrophotometer (BioDrop, UK). cDNA was synthesized from 2 μg of total RNA using Oligo-d$(T)_{15}$ primers and PrimeScript Reverse Transcriptase kit (Takara, Japan) according to the manufacturer's protocol. The cDNA products were amplified using following primers: iNOS (forward 5´-CTGCAGCACTTGGATCAGGAACCTG-3´, reverse 5´-GGGAGTAGCCTGTGTGCACCTGGAA-3´); TNF-*α* (forward 5´-

조선대학교
CHOSUN UNIVERSITY

CCTGTAGCCCACGTCGTAGC-3´, reverse 5´-TTGACCTCAGCGCTGAGTTG-3´) and GAPDH (forward 5´-GAGTCAACGGATTTGGTCGT-3´, reverse 5´-GACAAGCTTCCCGTTCTCAG-3´) (Jantaruk, Roytrakul, Sitthisak, & Kunthalert, 2017). The PCR amplification was carried out at initial denaturation at 94 ℃ for 5 min, followed by forty cycles of denaturation at 94 ℃ for 1 min, annealing at 55 ℃ for 120 sec and extension at 72 ℃ for 1 min, with a final extension at 72 ℃ for 5min. The PCR products were separated by electrophoresis and visualized under UV illumination.

2.13 LPS binding assay

The LPS-binding ability of TZP4 was determined by a BODIPY-TR-cadaverine (BC) displacement assay (Sautrey et al., 2014; Ma et al., 2015). Briefly, LPS from *E. coli* O111:B4 (25 μg/mL) was incubated with BC (2.5 μg/mL) and TZP4 or LL-37 (1-32 μg/mL) in Tris buffer (50 mM, pH 7.4) for 4 h. A volume of 2 mL of this mixture was added to a quartz cuvette. The fluorescence was recorded at an excitation wavelength of 580 nm and an emission wavelength of 620 nm with a Shimadzu RF-5301PC fluorescence spectrophotometer (Shimadzu Scientific Instruments, Kyoto, Japan). The percentage fluorescence was calculated using formula: $\%\Delta F\ (AU) = [(F_{obs}-F_0) / (F_{100}-F_0)] \times 100$, where F_{obs} is the observed fluorescence at a given peptide concentration, F_0 is the initial fluorescence of BC with LPS in the absence of peptides, and F_{100} is the BC fluorescence with LPS cells upon the addition of 10 μg/mL Polymyxin B.

조선대학교
CHOSUN UNIVERSITY

2.14 Dissociation of LPS-FITC aggregates

The ability of TZP4 to disaggregate FITC-conjugated LPS (Sigma, USA) oligomers was performed as described previously (Bhunia, Mohanram, & Bhattacharjya, 2009). Briefly, FITC-LPS (1 μg/mL) was added in a quartz cuvette containing 1×PBS and background fluorescence was measured at emission of 515 nm using 5301 PC Spectrofluorophotometer. The variations in emission of FITC after addition of different concentration of peptides was recorded (excitation λ = 488 nm, emission λ = 512 nm). The emissions of both PBS and peptides alone were taken as positive control. Dissociation of the aggregates of FITC-LPS results in an increase in the fluorescence of FITC because of dequenching (de Haas, van Leeuwen, Verhoef, van Kessel, & van Strijp, 2000). The changes in emissions were tracked until the system reached equilibrium.

2.15 Effect of TZP4 on LPS-FITC binding to RAW264.7 cells

Ability of TZP4 to bind with LPS-FITC on macrophage cells was performed as previously described (Rosenfeld, Papo, & Shai, 2006). Briefly, 1 μg/mL of LPS-FITC was incubated with TZP4 and LL-37 (10 μg/mL final concentration) for 1 h at 4 °C. This LPS-FITC/peptide mixture and untreated LPS-FITC was added to RAW264.7cells (5×10^5 cells/mL) and incubated at 37 °C for 30 min. The cells were then washed with ice cold PBS (pH 7.4) to remove the unbound LPS and the binding of FITC-LPS to RAW264.7 cells was analyzed by measuring median fluorescence intensity using flow cytometry (FACS Calibur, Beckman Coulter Inc., USA). Background fluorescence was assessed by using RAW 264.7 cells incubated without FITC-LPS or peptides. Background

조선대학교
CHOSUN UNIVERSITY

fluorescence was assessed by using RAW 264.7 cells incubated without FITC-LPS or peptides.

2.16 Statistical analysis

All data were analyzed by one-way analysis of variance (ANOVA) using SPSS 16.0 software. The data are presented as the means ± standard deviation from at least three independent experiments. The statistical significance was defined as a P-value of less than 0.05.

조선대학교
CHOSUN UNIVERSITY

3. Results

3.1 Activity against antibiotic-resistant bacterial strains

TZP4 (MIC: 16-64μg/ml) showed potent antimicrobial activity comparable to melittin (MIC: 8-32μg/ml) against antibiotic-resistant bacteria, such as methicillin-resistant *Staphylococcus aureus* (MRSA) and multidrug-resistant *Pseudomonas aeruginos*a (MDRPA) (Table 1). Three clinically used antibiotics (MIC: >128 μg/mL) including chloramphenicol, ciprofloxacin and oxacillin were less active to MRSA and MDRPA. However, ciprofloxacin (MIC: 32 μg/mL) was sensitive to one MDRPA strain (CCARM 2109).

3.2 Protease resistance

To determine its proteolytic stability, we incubated TZP4 with trypsin for the indicated time periods. Thereafter, the effect of the digestion against pepsin, trypsin, and α-chymotrypsin on the bactericidal activity of TZP4 against *Escherichia coli* was determined using the radial diffusion assay. As shown in Figure 2, the treatment of pepsin, trypsin, or α-chymotrypsin completely abolished the antimicrobial activity of melittin against *E. coli*. In contrast, the treatment of these three digestive enzymes had no effect on the antimicrobial activity of TZP4.

3.3 Drug resistance

We next investigated whether a reference strain of *S. aureus* (KCTC 1621) would evolve drug resistance after multiple exposures to TZP4 at 0.5 × MIC (Figure 3 & Table S1). After 15 passages, the MICs of TZP4 increased by 4-fold for *S. aureus*

조선대학교
CHOSUN UNIVERSITY

(KCTC 1621), while, the MICs of ciprofloxacin increased by 128-fold. This result indicated TZP4, unlike ciprofloxacin, could hardly develop drug resistance.

3.4 Bactericidal kinetics assay

The bactericidal kinetics of TZP4 against gram-negative and gram-positive bacteria were assessed using a time dependent killing kinetics assay. As depicted in Figure 4, the control peptide, melittin, rapidly killed both gram-negative and gram-positive bacteria in less than 10 min. However, TZP4 exhibited slower killing rates, requiring more than 1 h of exposure. This difference in killing profile may be attributed to the inability of TZP4 to lyse the bacterial membrane. These results suggested that TZP4 may mediate antimicrobial activity through a non-membrane-targeting mechanism.

3.5 Mechanism of antimicrobial action

To investigate the mechanism of the antimicrobial action of TZP4, its effect on the cytoplasmic membrane of bacterial cells was evaluated in membrane depolarization, SYTOX Green uptake, and flow cytometry experiments.

3.5.1 Cytoplasmic membrane depolarization

The membrane potential-sensitive dye, diSC_3-5, was used to measure the ability of TZP4 to depolarize the cytoplasmic membrane. Under conditions of normal potential across the membrane, the diSC_3-5 dye is distributed inside and outside of bacterial cells. Therefore, initially the fluorescence intensity of the dye decreases because of its self-quenching inside the bacterial cells. Upon disruption of the cytoplasmic membrane, diSC_3-5 is released into the culture media, leading to an

조선대학교
CHOSUN UNIVERSITY

increase in fluorescence intensity. As shown in Figure 5a, depolarization of the *S. aureus* membrane by the addition of TZP4 and peptides (final concentration: 2 × MIC) was monitored over a period of 500 s. Similar to buforin-2 (intracellular targeting AMP) treatment, TZP4 treatment inhibited depolarization and no changes in fluorescence intensity were seen. In contrast, the addition of melittin and LL-37 (membrane targeting AMP) induced rapid depolarization of the membrane in a manner similar to that of 0.1% Triton ×-100 (positive control). Additionally, membrane permeability was observed, even after the addition of increasing concentrations of TZP4 (1 × MIC, 2 × MIC, 4 × MIC, and 8 × MIC). As shown in Figure 5b, TZP4 failed to induce membrane depolarization even at 8 × MIC, further confirming its intracellular targeting properties. Also, similar to buforin-2, TZP4 did not depolarize membrane potential against *E. coli* even at 64 μg/ml (Figure S1).

3.5.2 SYTOX Green uptake assay

SYTOX Green uptake assays were performed to further examine the effects of TZP4 on bacterial membrane integrity. SYTOX Green is an asymmetrical cyanine dye that is unable to pass through intact cell membranes and its fluorescence increases significantly when bound to nucleic acids (Roth, Poot, Yue, & Millard, 1997). If the integrity of the cell membrane is compromised following exposure to the test compounds, SYTOX Green can enter the bacterial cell and bind to nucleic acids, resulting in an increase in fluorescence. As shown in Figure 5c, neither TZP4 nor buforin-2 treatment resulted in an increase in fluorescence intensity at any concentration tested, indicating the inability of these peptides to disrupt the membrane. In addition, the membrane disruption was observed while gradually increasing the concentration of TZP4 from 1 × MIC to 8 × MIC. As observed in

조선대학교
CHOSUN UNIVERSITY

buforin-2, TZP4 failed to disrupt the membrane even at 8 × MIC (Figure 5d). This observation was consistent with the results of membrane depolarization

3.5.3 Flow cytometric analysis

Flow cytometric analysis was performed to further characterize the membrane integrity of *E. coli* and *S. aureus* after TZP4 treatment. Propidium iodide (PI) fluorescently stains nucleic acids following cytoplasmic membrane disruption. In the absence of the peptide (control), only 0.73% and 1.14% of *E. coli* and *S. aureus* cells, respectively, exhibited PI fluorescent signal, indicating viable cell membranes (Figure 6). Treatment with melittin (membrane-targeting AMP) at 2 × MIC resulted in 70.47% and 78.13% of *E. coli* and *S. aureus* cells showing PI uptake, respectively. In contrast, the percentage of PI-positive *E. coli* and *S. aureus* cells after treatment with TZP4 at 2 × MIC, was only 4.29% and 2.42%, respectively. Similar results were observed with buforin-2, further confirming that TZP4 does not target bacterial cell membranes, but kills the bacteria via an intracellular-targeting mechanism.

3.5.4 DNA-binding activity

From these results, it was evident that TZP4 kills bacteria by targeting intracellular organelles, without disrupting the bacterial membrane. To determine the influence of TZP4 on plasmid DNA, retardation of the electrophoretic movement of plasmid DNA through an agarose gel (1%, w/v) was assessed after treatment with various concentrations of TZP4. As depicted in Figure 7, TZP4 and buforin-2 (DNA-binding peptide) completely inhibited DNA migration through the gel at a concentration of 32 μg/mL.

조선대학교
CHOSUN UNIVERSITY

3.5.5 Effects of TZP4 on RAW264.7 cell viability

Prior to investigating the inhibitory activity of TZP4 against LPS-induced inflammation, its cytotoxicity against the murine macrophage cell line, RAW264.7, was evaluated using the MTT assay, which is based on the reduction of 3-(4,5-dimethyl-2-thizolyl)-2,5-diphenyl-2H-tetrazolium bromide into a formazan dye by the mitochondria of living cells. TZP 4 showed low cytotoxicity, with cell viability up to 90% at the highest tested concentration of 64 μg/mL (Figure 8a).

3.5.6 Effects of TZP4 on LPS-induced NO and TNF-α production in RAW264.7 cells

NO and TNF-α are two important factors that are primarily involved in promoting inflammatory responses. To assess the effects of TZP4 on LPS-induced inflammation, its inhibitory activity against LPS-stimulated NO production was examined using the Griess assay. Similar to LL-37, 16 μg/mL TZP-4 significantly reduced LPS-induced NO production (Figure 8a). Next, the effect of TZP-4 on TNF-α production in LPS-stimulated RAW 264.7 cells was determined using a sandwich ELISA. Although somewhat weaker than LL-37, TZP-4 exhibited significant inhibitory activity against LPS-stimulated TNF-α production at 16 μg/mL (Figure 8b).

조선대학교
CHOSUN UNIVERSITY

3.6 Mechanism of anti-inflammatory activity

3.6.1 LPS-binding assay

LPS is the major cell wall component of gram-negative bacteria and it can induce severe endotoxemia when present at high concentrations in the blood. We assessed the direct LPS-binding ability of TZP4 using a fluorescence-based displacement assay with BODIPY-TR cadaverine (BC) (Figure 8d). Initially, BC fluorescence is quenched when it binds free LPS. The introduction of anti-endotoxin compounds displaces BC and its fluorescence increases, indicating successful binding of the compound with LPS. As shown in Figure 8d**,** TZP4 showed a concentration-dependent increase in fluorescence intensity, similar to that of LL-37, with almost 80% binding to LPS at 16 μg/mL.

3.6.2 Dissociation of LPS-FITC aggregates

LPS forms aggregates in aqueous suspension, which subsequently bind to LPS binding protein (LBP) and are transferred to CD14 receptors on the surface of macrophages. All endotoxin-neutralizing compounds are known to dissociate LPS aggregates (Wright, Tobias, Ulevitch, & Ramos, 1989). The ability of TZP4 to dissociate *E. coli* 0111:B4 LPS-FITC is shown in Figure 9a. Initially, the fluorescence of LPS-FITC aggregates was self-quenched, but the fluorescence intensity increased when the aggregates dissociated. Treatment with both TZP4 and LL-37 resulted in a dose-dependent increase in fluorescence intensity. Notably, TZP4 showed a greater effect at dissociating LPS-FITC aggregates at lower concentrations than LL-37, a well-studied LPS neutralizer.

조선대학교
CHOSUN UNIVERSITY

3.6.3 Effect of TZP4 on the binding of LPS-FITC to RAW264.7 macrophages

We investigated the effects of TZP4 and LL-37 on the binding of LPS-FITC to RAW264.7 cells using flow cytometry. As shown in Figure 9b, when RAW264.7 cells were incubated with *E. coli* LPS-FITC, in the absence of TZP4 and LL-37, FITC fluorescence was observed in 63.6% of cells. In contrast, when LPS-FITC was pre-incubated with TZP4 or LL-37, FITC fluorescence was markedly suppressed to 17.6% and 12.4% of cells, respectively. These observations further confirmed the successful binding of TZP4 to LPS.

조선대학교
CHOSUN UNIVERSITY

4. Discussion

Thirteen TZPs consisting of cationic and hydrophobic moieties were previously designed (Gunasekaran, et al., 2019). These polymers were active against standard gram-positive and gram-negative bacterial strains. Of these polymers, TZP4, which has the lowest molecular weight and exhibits the highest cell selectivity (indicative of therapeutic index), was chosen as the optimal lead polymer for the present study. Furthermore, TZP4 displayed potent antimicrobial activity against different antibiotic-resistant pathogens, such as MRSA and MDRPA (Table1).

It is well known that poor tolerance to proteases has always been an insurmountable obstacle to the clinical application of AMPs. Therefore, it is also important to assess the interference effects of gastric enzymes and pancreatic enzymes on antimicrobial activity of TZP4, such as pepsin, trypsin and α-chymotrypsin (Low 1982). In this study, the susceptibility of TZP4 to proteolysis by these enzymes were investigated. Our results revealed that TZP4 is resistant to proteolytic digestion by these enzymes (Figure 2).

The low possibility of emerging antibiotic resistance is one of the important factors to have as alternative therapeutic agents for conventional antibiotics (Spohn et al., 2019). Therefore, we here investigated whether a reference strain of *S aureus* would evolve resistance after multiple exposures to TZP4 at 0.5 × MIC. TZP4 still remained highly sensitive to bacterial strains after 12 passages (Figure 3). The MICs of TZP4 increased up to 4-fold its initial MIC at 12th passage. In contrast, ciprofloxacin, an antibiotic acting against topoisomerase IV and DNA gyrase reached an MIC 128-fold greater than its initial MIC at 12th passage. TZP4 had a considerably lower potential for inducing resistance than conventional

조선대학교
CHOSUN UNIVERSITY

antibiotic. Therefore, lower emergence of antibiotic resistance and proteolytic resistance of TZP4 suggested that it can be a potential candidate for use in clinical therapy.

Despite its effective antimicrobial activity, TZP4 exerted a slower killing rate compared to melittin (Figure 4). These observations suggest that the bactericidal mechanism of TZP4 was different from that of melittin. The predominant mechanism of AMPs, such as melittin and LL-37, lies in their binding to and rapid perturbation of bacterial membranes, which leads to cell death via the leakage of cytoplasmic contents (Oren & Shai, 1998). However, some AMPs, such as buforin-2 and indolicidin, have been reported to kill bacteria by translocating across the bacterial membrane without disrupting it and binding to DNA, thereby inhibiting DNA, RNA, and protein synthesis. Therefore, to gain further insights into the mechanism of the antimicrobial action of TZP4, various fluorochrome-based studies, including cytoplasmic membrane depolarization, SYTOX Green uptake, and flow cytometry assays were performed. Membrane-lysing peptides, such as melittin and LL-37 and the membrane-penetrating peptide, buforin-2, were used as controls. These results revealed, that similar to buforin-2 (a well-studied intracellular-targeting AMP), TZP4 did not induce damage to the membrane permeability or integrity of *S. aureus* and *E. coli* bacteria (Figures 5 and 6) at 2 × MIC, suggesting that the cytoplasmic membrane of the bacterial cell is not the ultimate target of TZP4. Furthermore, gel retardation assays revealed that TZP4 bound to *E. coli* DNA at 32μg/mL, confirming that it had similar intracellular targeting properties to buforin-2 (Figure 7). Collectively, these findings indicated that the mode of antimicrobial action of TZP4 involved targeting intracellular organelles rather than the bacterial membrane.

조선대학교
CHOSUN UNIVERSITY

LPS is a major constituent of the outer membrane leaflet of gram-negative bacteria. It is released spontaneously and rapidly during bacterial growth and after antibiotic exposure (Jackson & Kropp, 1992; van Langevelde et al., 1998). LPS is a strong immunostimulant that can stimulate immunocytes, such as macrophages, monocytes, and neutrophils to release inflammatory cytokines (e.g., TNF-α) via the formation of LPS-CD14 complexes (Hancock, Haney, & Gill, 2016; Rosenfeld, Papo, & Shai, 2006). LPS binds to toll-like receptor 4 (TLR4) receptors on the cell surface, triggering the secretion of various inflammatory factors that contribute to the pathophysiology of septic shock or sepsis *in vivo* (Lakhani, & Bogue, 2003; Miyake, 2004; Munford, 2005). The standard treatment for sepsis and endotoxicity is the use of antibiotics (Brandenburg, & Schürholz, 2015; Vianna et al., 2004; Vincent, Pereira, Gleeson, & De Backer, 2014); however, this strategy has drawbacks. In particular, when antibiotics kill bacteria, they simultaneously induce the release of LPS. Although the known LPS-binding inhibitor, polymyxin B, can neutralize LPS during the process of killing bacteria, its clinical applications are limited due to its neurological and renal toxicity. Thus, the development of new antibiotics capable of neutralizing LPS is urgently needed (Acuña et al., 2016; Salazar, Alarcón, Huerta, Navarro, & Aguayo, 2017; Jantaruk, P, Roytrakul, Sitthisak, & Kunthalert, 2017).

NO and TNF-α are typical inflammatory mediators secreted by LPS-activated macrophages. TNF-α mediates septic shock in chronic infections (Beutler, Milsark, & Cerami, 1985). The increased production of NO by iNOS has been associated with various disorders, such as septic shock, rheumatoid arthritis, and chronic infection (Chakravortty, & Kumar, 1997). Accordingly, we observed the effects of TZP4 on NO and TNF-α levels in RAW264.7 cells stimulated with LPS. TZP4 was

조선대학교
CHOSUN UNIVERSITY

significantly decreased the mRNA levels of iNOS and TNF-α and inhibited NO and TNF-*α* release from RAW264.7 cells stimulated with LPS (Figure 8b & 8c). These results strongly suggested that TZP4 may be involved in the downregulation of pro-inflammatory mediator production and inhibit inflammation in gram-negative bacterial infections.

The primary aim of this study was to investigate the mechanism underlying the endotoxin-neutralizing activity of TZP4. Here, we found that TZP4 directly bound to *E. coli* LPS, using a BC displacement assay (Figure 8d). BC binds strongly to lipid-A moiety domains of LPS. TZP4 displaces the BC probe and binds to LPS, which eventually leads to an increase in fluorescence from free BC. Previous studies have suggested that LPS only induces an inflammatory response when it is in an aggregated form (oligomer) (Mueller et al., 2004). It is important for any anti-endotoxin agent to dissociate these LPS aggregates and block them from binding to LBP (Rosenfeld, Papo, & Shai, 2006). However, not all LPS-binding compounds possess the ability to disaggregate LPS. In the present study, we observed that TZP4 more efficiently induced the disaggregation of LPS-FITC at lower concentrations, compared to LL-37 (Figure 9a). Previous studies have shown that LPS-binding AMPs, such as magainin-2, fail to detoxify the inflammatory response, despite their high affinity towards LPS (Rosenfeld, Papo, & Shai, 2006). This has led to the speculation that strong binding with LPS alone is not sufficient to block the biological activity of LPS. Monocytes or macrophages induce an inflammatory response when LPS binds to its cell surface receptor, CD14. This receptor-bound LPS in turn binds to TLR4 and induces the release of pro-inflammatory cytokines. Various studies have demonstrated that LPS interacts with CD14 receptors by direct binding or via LBP (Mookherjee, & Hancock, 2007; Nan, Bang, Jacob, Park, &

조선대학교
CHOSUN UNIVERSITY

Shin, 2012; Suzuki et al., 2011). Therefore, it is believed that inhibiting the interaction between LPS and the CD14 receptor is important for preventing the activation of macrophages. Flow cytometric analysis showed that pre-incubation of FITC-conjugated LPS with TZP4 greatly inhibited its binding to RAW264.7 cells, to a similar extent as the anti-endotoxin AMP, LL-37 (Moffatt et al., 2013; Nagaoka et al., 2001) (Figure 9b). Collectively, these findings indicated that TZP4 has dual abilities to neutralize LPS and exert anti-endotoxic activity, either by blocking the direct interaction of LPS with LBP or by inhibiting the binding of LPS to the CD14 receptor. We further evaluated the cytotoxicity of TZP4 against RAW 264.7 cells and found that cell viability exceeded 95% at a TZP4 concentration of 64 μg/mL (Figure 8a). Therefore, the LPS-neutralizing property of TZP4 was independent of its effect on cell viability, indicating its suitability as novel LPS-neutralizing agent.

조선대학교
CHOSUN UNIVERSITY

5. Conclusion

The present study is the first to report the mechanism of the antimicrobial action and LPS-neutralizing activity of a triazine-based amphipathic polymer, TZP4. Besides its direct antimicrobial activity, TZP4 exhibited potent anti-endotoxin activity. These antimicrobial and anti-endotoxin properties make TZP4 a promising drug candidate for the treatment of endotoxic shock and sepsis caused by gram-negative bacterial infections.

조선대학교
CHOSUN UNIVERSITY

Table 1. Antimicrobial activities of TZP4, melittin and conventional antibiotics against antibiotic-resistant bacterial strains

Bacterial strains	MIC (μg/mL)				
	TZP4	melittin	chloramphenicol	ciprofloxacin	oxacillin
MRSA[a]					
CCARM 3089	16	8	512	256	256
CCARM 3090	16	16	256	>1024	1024
MDRPA[b]					
CCARM 2095	32	32	128	256	1024
CCARM 2109	64	32	>1024	32	>1024

[a] MRSA: methicillin-resistant *Staphylococcus aureus*
[b] MDRPA: multidrug-resistant *Pseudomonas aeruginosa*

조선대학교
CHOSUN UNIVERSITY

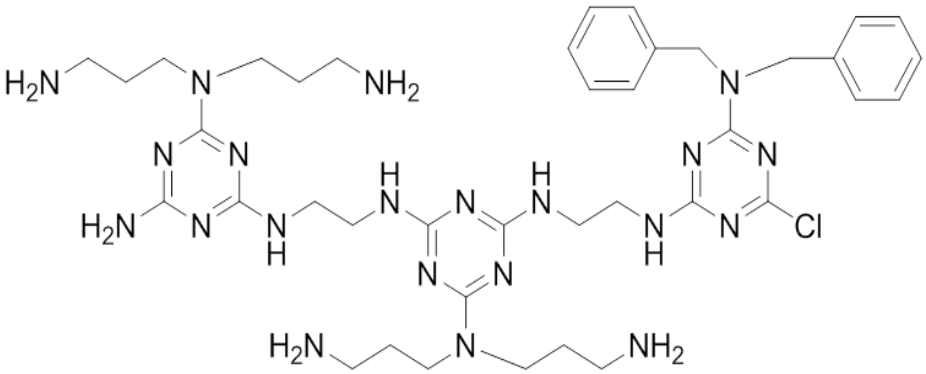

Figure 1. Structure of the triazine-based amphipathic polymer, TZP4

조선대학교
CHOSUN UNIVERSITY

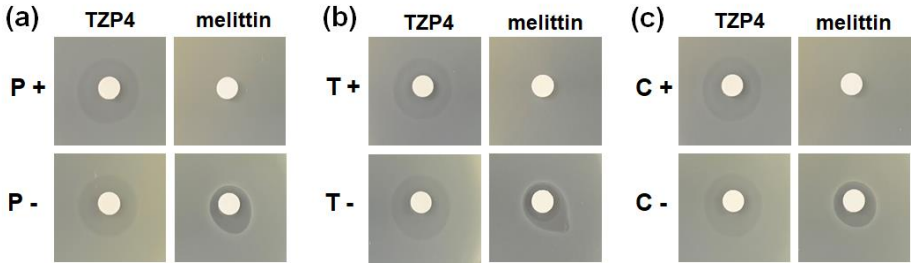

Figure 2. Inhibition of antimicrobial activity of TZP4 and melittin by pepsin (a), trypsin (b), and α-chymotrypsin (c), as assessed by a radial diffusion assay using *E. coli* (KCTC 1682). P, T and C represent pepsin, trypsin, and α-chymotrypsin, respectively.

조선대학교
CHOSUN UNIVERSITY

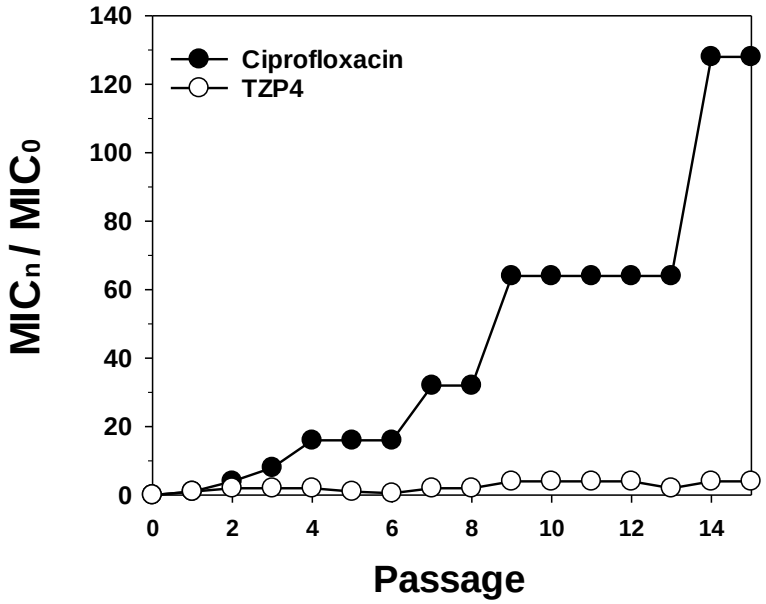

Figure 3. Drug resistance development of *S. aureus* (KCTC 1621) in the presence of sub-MIC concentration of TZP4 and ciprofloxacin.

조선대학교
CHOSUN UNIVERSITY

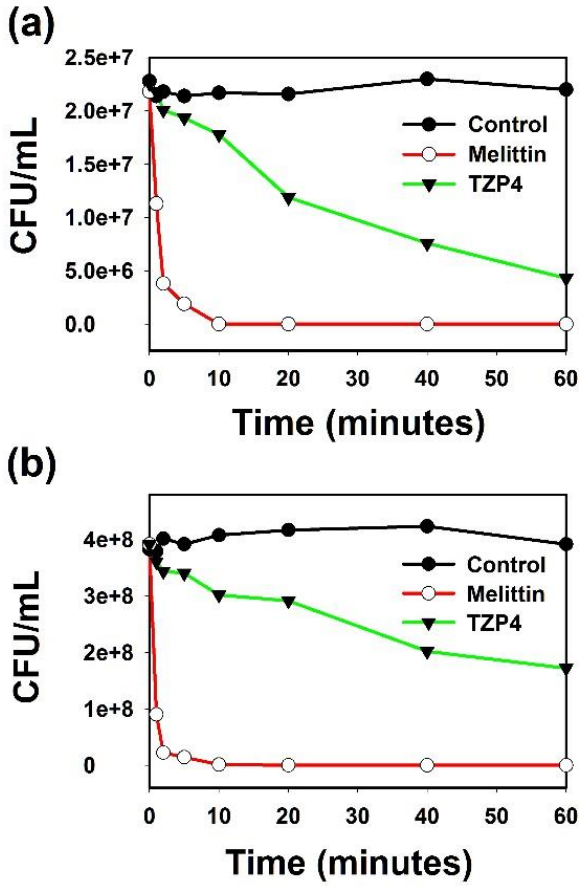

Figure 4. Time-killing kinetics of TZP4 (1 × MIC) against (a) gram-negative *E. coli* and (b) gram-positive *S. aureus*. CFU, colony-forming units.

조선대학교
CHOSUN UNIVERSITY

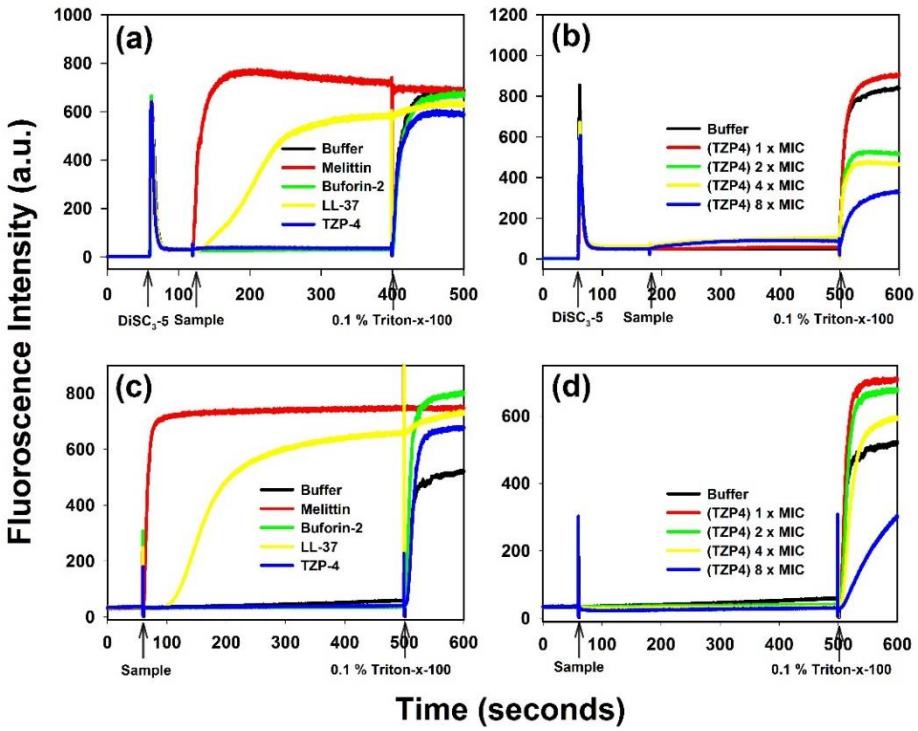

Figure 5. Time-dependent cytoplasmic membrane depolarization of *S. aureus* (KCTC 1621) treated with (a) 2 × MIC of TZP4 and (b) increasing concentrations of TZP4, as assessed by the release of the membrane potential-sensitive dye, $DiSC_3$-5. SYTOX Green uptake by *S. aureus* (KCTC 1621) treated with (c) 2 × MIC of TZP4 and (d) increasing concentrations of TZP4. Cytoplasmic membrane alterations allow the SYTOX Green probe to enter the cell and bind DNA, resulting in an increase in fluorescence. Triton X-100 (0.1%) was added to achieve complete permeabilization.

조선대학교
CHOSUN UNIVERSITY

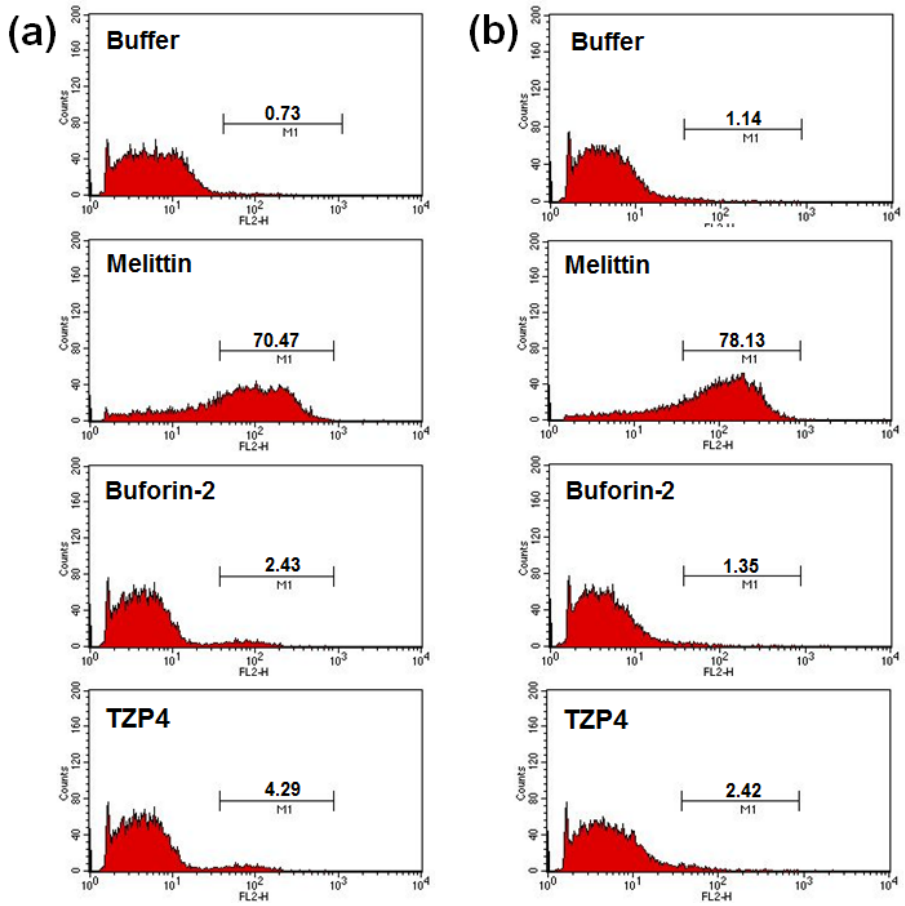

Figure 6. Membrane integrity of (a) *E. coli* (KCTC 1682) and (b) *S. aureus* (KCTC 1621), as observed by flow cytometry. The mid-logarithmic phase of bacterial culture was treated with 2 × MIC of TZP4 or peptides, and cellular fluorescence was observed using a FACS scan flow cytometer. Membrane damage was measured as the increase in propidium iodide (10 μg/mL) fluorescence intensity after 1 h at 37 ℃.

조선대학교
CHOSUN UNIVERSITY

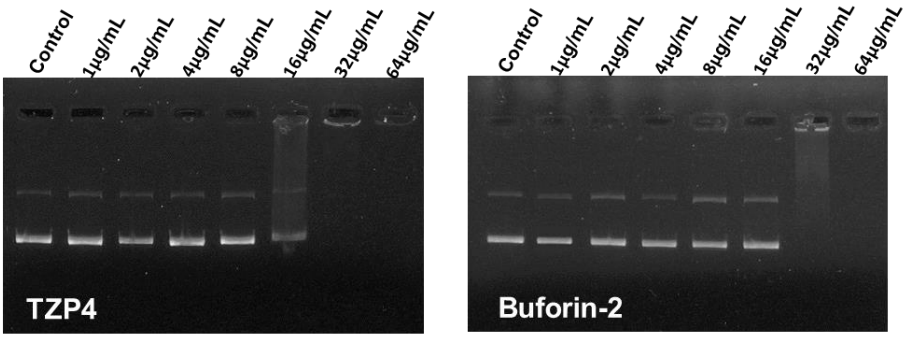

Figure 7. DNA-binding activity. Plasmid DNA (100 ng; pBR322) and peptides were co-incubated for 1 h. DNA migration at the indicated peptide concentration (1 to 64 μg/mL) was determined by gel retardation assay.

조선대학교
CHOSUN UNIVERSITY

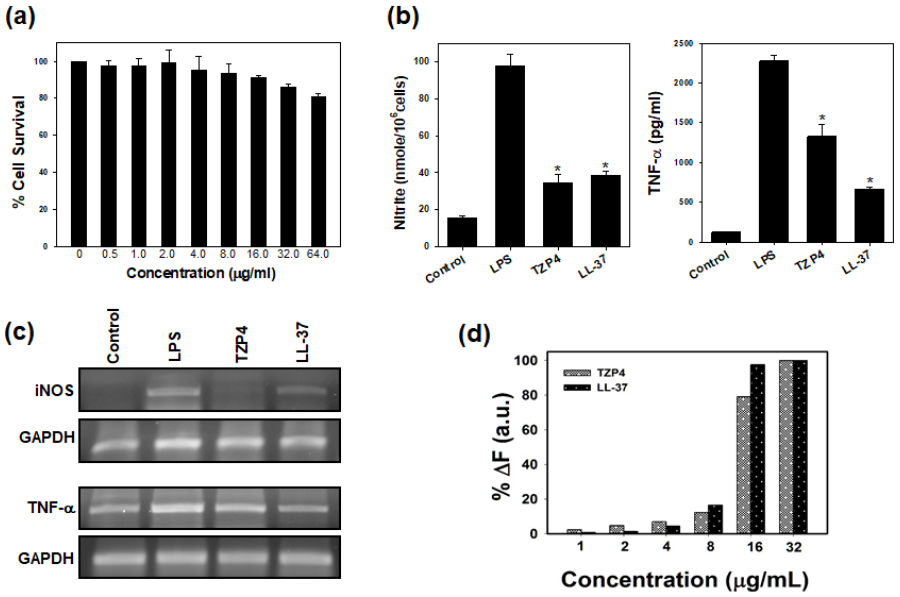

Figure 8. (a) MTT assay of TZP4 cytotoxicity against RAW 264.7 macrophages. (b) Effects of TZP4 (16 μg/mL) and LL-37 (16 μg/mL) on NO and TNF-α release from LPS-stimulated RAW264.7 cells. (c) Effects of TZP4 (16 μg/mL) and LL-37 (16μg/mL) on iNOS and TNF-α mRNA expression in LPS-stimulated RAW 264.7 cells. Asterisks indicate significant effects compared to LPS-treated cells. All data were analyzed using a one-way ANOVA, with Bonferroni's post-test (*$P < 0.001$ for each agonist). (d) Binding ability of TZP4 and LL-37 to LPS from *E. coli* 0111:B4. The fluorescence intensity was monitored at an excitation wavelength of 580 nm and an emission wavelength of 620 nm.

조선대학교
CHOSUN UNIVERSITY

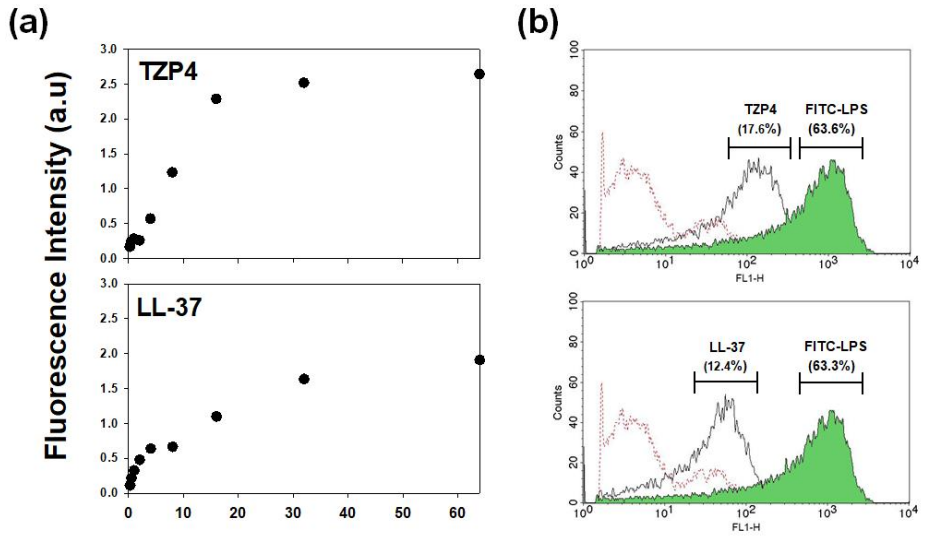

Figure 9. (a) Dissociation of *E. coli* 0111:B4 LPS-FITC aggregates in the presence of increasing concentrations of TZP4 and LL-37. The change in FITC fluorescence after each treatment was monitored until it reached equilibrium. FITC fluorescence increased as the distance between its monomers increased, because of self-quenching. (b) Effects of TZP4 and LL-37 on the binding of LPS-FITC to RAW264.7 macrophages. LPS-FITC (*E. coli* 0111:B4, 1 μg/mL) was incubated with TZP4 (10 μg/mL) or LL-37 (10 μg/mL) for 1 h and then added to RAW264.7 cells (5×10^5 cells/mL) and further incubated for 30 min. The cells were washed and the binding of LPS-FITC to macrophages was analyzed using a FACSCalibur flow cytometer. Values given with the peaks represent the mean fluorescence intensity of the cell bound to FITC-LPS. The red dotted line indicates the background fluorescence of untreated cells.

조선대학교
CHOSUN UNIVERSITY

References

[1] Acuña, L. G., Barros, M. J., Peñaloza, D., Rodas, P. I., Paredes-Sabja, D., Fuentes, J. A., Gil, F., Calderón, I. L. (2016). A feed-forward loop between SroC and MgrR small RNAs modulates the expression of eptB and the susceptibility to polymyxin B in Salmonella Typhimurium. *Microbiology, 162(11),* 1996–2004.

[2] Ahn, M., Gunasekaran, P., Rajasekaran, G., Kim, E. Y., Lee, S. J., Bang, G., Cho, K., Hyun. J. K., Lee, H. J., Jeon, Y. H., Kim, N. H., Ryu, E. K., Shin, S. Y., Bang, J. K. (2017) Pyrazole Derived Ultra-Short Antimicrobial Peptidomimetics With Potent Anti-Biofilm Activity. *European Journal of Medicinal Chemistry, 125*, 551–564

[3] Beutler, B., Milsark, I.W., Cerami, A. C., 1985. Passive immunization against cachectin/tumor necrosis factor protects mice from lethal effect of endotoxin. *Science,* 229, 869–871.

[4] Bhunia, A., Mohanram, H., & Bhattacharjya, S. (2009). Lipopolysaccharide bound structures of the active fragments of fowlicidin-1, a cathelicidin family of antimicrobial and antiendotoxic peptide from chicken, determined by transferred nuclear overhauser effect spectroscopy. *Biopolymers, 92(1)*, 9–22.

[5] Brandenburg, K., & Schürholz, T. (2015). Lack of new antiinfective agents: Passing into the pre-antibiotic age? *World Journal of Biological Chemistry, 6(3)*, 71

[6] Chakravortty, D., & Kumar, K. S. N., (1997) Induction of cell proliferation and collagen synthesis in human small intestinal lamina propria fibroblasts by lipopolysaccharide: possible involvement of nitric oxide. *Biochemical Biophysics Research Communation*, *240(2)*, 458–463

조선대학교
CHOSUN UNIVERSITY

[7] Chou, S., Shao, C., Wang, J., Shan, A., Xu, L., Dong, N., & Li, Z. (2016). Short, multiple-stranded β-hairpin peptides have antimicrobial potency with high selectivity and salt resistance. *Acta Biomaterialia, 30*, 78–93.

[8] de Haas, C. J., van Leeuwen, H. J., Verhoef, J., van Kessel, K. P., & van Strijp, J. A. (2000). Analysis of lipopolysaccharide (LPS)-binding characteristics of serum components using gel filtration of FITC-labeled LPS. *Journal of Immunological Methods, 242(1-2),* 79–89.

[9] Dong, N., Ma, Q., Shan, A., Lv, Y., Hu, W., Gu, Y., & Li, Y. (2012). Strand length-dependent antimicrobial activity and membrane-active mechanism of arginine-and valine-rich β-hairpin-like antimicrobial peptides. *Antimicrobial Agents and Chemotherapy, 56(6),* 2994–3003.

[10] Giamarellou, H. (2006) Treatment options for multidrug-resistant bacteria. *Expert Review of Anti-infective Therapy*, *4(4)*, 601–618.

[11] Ghosh, C., & Haldar. J. (2015) Membrane-Active Small Molecules: Designs Inspired by Antimicrobial Peptides. *ChemMedChem 10(10),* 1606–1624.

[12] Gunasekaran, P., Fan, M., Kim, E. Y., Shin, J. H., Lee, J. E., Son, E. J., Kim, J., Hwang E, Yim MS, Kim EH, Choi, Y.-J., Lee, Y. H., Chung, Y. H., Kim, H. N., Ryu, K., Shin. S. Y., Kim. E. K., & Bang. J. K. (2019). Amphiphilic Triazine Polymer Derivatives as Antibacterial And Anti-atopic Agents in Mice Model. *Scientific Reports, 9(1)*, 15161.

[13] Hancock, R. E., Haney, E. F., Gill, E. E. (2016) The immunology of host defence peptides: beyond antimicrobial activity. *Nature Review Immunology 16(5)*, 321−334.

[14] Jackson, J. J., & Kropp, H. (1992). ß-Lactam antibiotic-induced release of

조선대학교
CHOSUN UNIVERSITY

free endotoxin: in vitro comparison of penicillin-binding protein (PBP) 2-specific imipenem and PBP 3-specific ceftazidime. *Journal of Infectious Diseases, 165(6)*, 1033−1041.

[15] Jantaruk, P., Roytrakul, S., Sitthisak, S., & Kunthalert, D. (2017) Potential role of an antimicrobial peptide, KLK in inhibiting lipopolysaccharide-induced macrophage inflammation. *PLoS One, 12(8)*, e0183852.

[16] Koh, J.-J., Qiu, S., Zou, H., Lakshminarayanan, R., Li, J., Zhou, X., Tang, C., Saraswathi, P., Verma, C., Tan, D. T. H., Tan, A. L., Liu, S., Beuerman, R. W. Tan, D. T. H., Tan, A. L., Liu, S. (2013). Rapid bactericidal action of alpha-mangostin against MRSA as an outcome of membrane targeting. *Biochimica et Biophysica Acta (BBA)-Biomembranes, 1828*(2), 834–844.

[17] Lakhani, S. A., & Bogue, C. W. (2003). Toll-like receptor signaling in sepsis. *Current Opinion in Pediatrics, 15*(3), 278–282.

[18] Low, A. G. (1982) The activity of pepsin, chymotrypsin and trypsin during 24 h periods in the small intestine of growing pigs. *British Journal of Nutrition, 48(1),* 147–159.

[19] Lyu, Y., Yang, Y., Lyu, X., Dong, N., & Shan, A. (2016) Antimicrobial activity, improved cell selectivity and mode of action of short PMAP-36-derived peptides against bacteria and Candida. *Scientific Reports, 6*, 27258

[20] Lyu, Y., Yang, X., Goswami, S., Gorityala, B.K., Idowu, T., Domalaon, R., Zhanel, G.G., Shan, A., & Schweizer, F. (2017) Amphiphilic tobramycin-lysine conjugates sensitize multidrug resistant gram-negative bacteria to rifampicin and minocycline. *Journal of Medicinal Chemistry 60,* 3684–3702.

[21] Ma, Z., Wei, D., Yan, P., Zhu, X., Shan, A., & Bi, Z. (2015). Characterization of cell selectivity, physiological stability and endotoxin

조선대학교
CHOSUN UNIVERSITY

neutralization capabilities of α-helix-based peptide amphiphiles. *Biomaterials, 52*, 517–530.

[22] Marín-Medina, N., Ramírez, D. A., Trier, S., & Leidy, C. (2016) Mechanical Properties That Influence Antimicrobial Peptide Activity in Lipid Membranes. *Applied Microbiology and Biotechnololgy*, *100(24)*, 10251−10263.

[23] Miyake, K. (2004). Endotoxin recognition molecules MD-2 and toll-like receptor 4 as potential targets for therapeutic intervention of endotoxin shock. *Current Drug Targets-Inflammation & Allergy, 3(3)*, 291−297.

[24] Moffatt, J. H., Harper, M., Mansell, A., Crane, B., Fitzsimons, T. C., Nation, R. L., Li, J., Adler, B., & Boyce, J. D. (2013). Lipopolysaccharide-deficient Acinetobacter baumannii shows altered signaling through host Toll-like receptors and increased susceptibility to the host antimicrobial peptide LL-37. *Infection and Immunity, 81(3)*, 684−689.

[25] Mookherjee, N., & Hancock, R. (2007). Cationic host defence peptides: innate immune regulatory peptides as a novel approach for treating infections. *Cellular and Molecular Life Sciences, 64(7-8)*, 922–933.

[26] Mueller, M., Lindner, B., Kusumoto, S., Fukase, K., Schromm, A. B., & Seydel, U. (2004). Aggregates are the biologically active units of endotoxin. *Journal of Biological Chemistry, 279(25)*, 26307–26313.

[27] Munford, R. S. (2005). Invited review: detoxifying endotoxin: time, place and person. *Journal of Endotoxin Research, 11(2),* 69–84.

[28] Nagaoka, I., Hirota, S., Niyonsaba, F., Hirata, M., Adachi, Y., Tamura, H., & Heumann, D. (2001). Cathelicidin family of antibacterial peptides CAP18 and CAP11 inhibit the expression of TNF-α by blocking the binding of LPS to CD14+ cells. *The Journal of Immunology, 167(6)*, 3329–3338

조선대학교
CHOSUN UNIVERSITY

[29] Nan, Y. H., Bang, J.-K., Jacob, B., Park, I.-S., & Shin, S. Y. (2012). Prokaryotic selectivity and LPS-neutralizing activity of short antimicrobial peptides designed from the human antimicrobial peptide LL-37. *Peptides, 35(2)*, 239–247.

[30] Oren, Z., Shai, Y. (1998) Mode of Action of Linear Amphipathic α-Helical Antimicrobial Peptides. *Biopolymers, 47(6)*, 451–463.

[31] Pollard. J. E., Snarr, J., Chaudhary, V., Jennings, J. D., Shaw, H., Christiansen, B., Wright, J., Jia, W., Bishop, R. E., Savage, P. B. (2012) In vitro evaluation of the potential for resistance development to ceragenin CSA-13. *Journal of Antimicrobial Chemotherapy, 67(11)*, 2665–2672.

[32] Rosenfeld, Y., Papo, N., & Shai, Y. (2006). Endotoxin (lipopolysaccharide) neutralization by innate immunity host-defense peptides peptide properties and plausible modes of action. *Journal of Biological Chemistry, 281(3)*, 1636–1643.

[33] Roth, B. L., Poot, M., Yue, S. T., & Millard, P. J. (1997) Bacterial viability and antibiotic susceptibility testing with SYTOX green nucleic acid stain. *Applied and Environmental Microbiology, 63(6)*, 2421–2431.

[34] Salazar, J., Alarcón, M., Huerta, J., Navarro, B., & Aguayo, D. (2017) Phosphoethanolamine addition to the Heptose I of the Lipopolysaccharide modifies the inner core structure and has an impact on the binding of Polymyxin B to the *Escherichia coli* outer membrane. *Archives of Biochemistry and Biophysics, 620*, 28–34.

[35] Sautrey, G., Zimmermann, L., Deleu, M., Delbar, A., Machado, L. S., Jeannot, K., Bambeke, F. V., Buyck, J. M., Decout, J-L., Mingeot-Leclercq, M.-P. (2014). New amphiphilic neamine derivatives active against resistant Pseudomonas aeruginosa and their interactions with lipopolysaccharides.

조선대학교
CHOSUN UNIVERSITY

Antimicrobial Agents and Chemotherapy, 58(8), 4420–4430.

[36] Spohn, R., Daruka, L., Lázár, V., Martins, A., Vidovics, F., Grezal, G., Méhi, O., Kintses, B., Számel, M., Jangir, P. K., Csörgő, B., Györkei, A., Bódi, Z., Faragó, A., Bodai, L., Földesi , I., Kata, D., Maróti G., Pap, B., Wirth, R., Papp, B., & Pál, C. (2019) Integrated evolutionary analysis reveals antimicrobial peptides with limited resistance. *Nature Communication 10(1)*, 4538.

[37] Suzuki, K., Murakami, T., Kuwahara-Arai, K., Tamura, H., Hiramatsu, K., & Nagaoka, I. (2011). Human anti-microbial cathelicidin peptide LL-37 suppresses the LPS-induced apoptosis of endothelial cells. *International Immunology, 23(3)*, 185–193.

[38] van Langevelde, P., Kwappenberg, K. M., Groeneveld, P. H., Mattie, H., & van Dissel, J. T. (1998). Antibiotic-induced lipopolysaccharide (LPS) release from Salmonella typhi: delay between killing by ceftazidime and imipenem and release of LPS. *Antimicrobial Agents and Chemotherapy, 42(4)*, 739–743

[39] Vianna, R. C., Gomes, R. N., Bozza, F. A., Amâncio, R. T., Bozza, P. T., David, C. M., & Castro-Faria-Neto, H. C. (2004). Antibiotic treatment in a murine model of sepsis: impact on cytokines and endotoxin release. *Shock, 21(2)*, 115–120.

[40] Vincent, J.-L., Pereira, A. J., Gleeson, J., & De Backer, D. (2014). Early management of sepsis. *Clinical and Experimental Emergency Medicine, 1(1)*, 3–7.

[41] Walsh, C. T., Wencewicz, T. A. (2014) Prospects for new antibiotics: a molecule centered perspective. *Journal of Antibiotis (Tokyo), 67(1)*, 7–22.

[42] Wang, J., Chou, S., Yang, Z., Yang, Y., Wang, Z., Song, J., Dou, X., Shan,

조선대학교
CHOSUN UNIVERSITY

A. (2018). Combating drug-resistant fungi with novel imperfectly amphipathic palindromic peptides. *Journal of Medicinal Chemistry, 61(9)*, 3889–3907.

[43] Acuña, L. G., Barros, M. J., Peñaloza, D., Rodas, P. I., Paredes-Sabja, D., Fuentes, J. A., Gil, F., Calderón, I. L. (2016). A feed-forward loop between SroC and MgrR small RNAs modulates the expression of eptB and the susceptibility to polymyxin B in Salmonella Typhimurium. *Microbiology, 162(11),* 1996–2004.

[44] Ahn, M., Gunasekaran, P., Rajasekaran, G., Kim, E. Y., Lee, S. J., Bang, G., Cho, K., Hyun. J. K., Lee, H. J., Jeon, Y. H., Kim, N. H., Ryu, E. K., Shin, S. Y., Bang, J. K. (2017) Pyrazole Derived Ultra-Short Antimicrobial Peptidomimetics With Potent Anti-Biofilm Activity. *European Journal of Medicinal Chemistry, 125*, 551–564

[45] Beutler, B., Milsark, I.W., Cerami, A. C., 1985. Passive immunization against cachectin/tumor necrosis factor protects mice from lethal effect of endotoxin. *Science,* 229, 869–871.

[46] Bhunia, A., Mohanram, H., & Bhattacharjya, S. (2009). Lipopolysaccharide bound structures of the active fragments of fowlicidin-1, a cathelicidin family of antimicrobial and antiendotoxic peptide from chicken, determined by transferred nuclear overhauser effect spectroscopy. *Biopolymers, 92(1)*, 9–22.

[47] Brandenburg, K., & Schürholz, T. (2015). Lack of new antiinfective agents: Passing into the pre-antibiotic age? *World Journal of Biological Chemistry, 6(3)*, 71.

[48] Chakravortty, D., & Kumar, K. S. N., (1997) Induction of cell proliferation and collagen synthesis in human small intestinal lamina propria fibroblasts by

조선대학교
CHOSUN UNIVERSITY

lipopolysaccharide: possible involvement of nitric oxide. *Biochemical Biophysics Research Communation*, *240(2)*, 458–463.

[49] Chou, S., Shao, C., Wang, J., Shan, A., Xu, L., Dong, N., & Li, Z. (2016). Short, multiple-stranded β-hairpin peptides have antimicrobial potency with high selectivity and salt resistance. *Acta Biomaterialia, 30*, 78–93.

[50] de Haas, C. J., van Leeuwen, H. J., Verhoef, J., van Kessel, K. P., & van Strijp, J. A. (2000). Analysis of lipopolysaccharide (LPS)-binding characteristics of serum components using gel filtration of FITC-labeled LPS. *Journal of Immunological Methods, 242(1-2),* 79–89.

[51] Dong, N., Ma, Q., Shan, A., Lv, Y., Hu, W., Gu, Y., & Li, Y. (2012). Strand length-dependent antimicrobial activity and membrane-active mechanism of arginine-and valine-rich β-hairpin-like antimicrobial peptides. *Antimicrobial Agents and Chemotherapy, 56(6),* 2994–3003.

[52] Giamarellou, H. (2006) Treatment options for multidrug-resistant bacteria. *Expert Review of Anti-infective Therapy*, *4(4)*, 601–618.

[53] Ghosh, C., & Haldar. J. (2015) Membrane-Active Small Molecules: Designs Inspired by Antimicrobial Peptides. *ChemMedChem 10(10),* 1606–1624.

[54] Gunasekaran, P., Fan, M., Kim, E. Y., Shin, J. H., Lee, J. E., Son, E. J., Kim, J., Hwang E, Yim MS, Kim EH, Choi, Y.-J., Lee, Y. H., Chung, Y. H., Kim, H. N., Ryu, K., Shin. S. Y., Kim. E. K., & Bang. J. K. (2019). Amphiphilic Triazine Polymer Derivatives as Antibacterial And Anti-atopic Agents in Mice Model. *Scientific Reports, 9(1)*, 15161.

[55] Hancock, R. E., Haney, E. F., Gill, E. E. (2016) The immunology of host defence peptides: beyond antimicrobial activity. *Nature Review Immunology*

조선대학교
CHOSUN UNIVERSITY

16(5), 321−334.

[56] Jackson, J. J., & Kropp, H. (1992). ß-Lactam antibiotic-induced release of free endotoxin: in vitro comparison of penicillin-binding protein (PBP) 2-specific imipenem and PBP 3-specific ceftazidime. *Journal of Infectious Diseases, 165(6)*, 1033−1041.

[57] Jantaruk, P., Roytrakul, S., Sitthisak, S., & Kunthalert, D. (2017) Potential role of an antimicrobial peptide, KLK in inhibiting lipopolysaccharide-induced macrophage inflammation. *PLoS One, 12(8)*, e0183852.

[58] Koh, J.-J., Qiu, S., Zou, H., Lakshminarayanan, R., Li, J., Zhou, X., Tang, C., Saraswathi, P., Verma, C., Tan, D. T. H., Tan, A. L., Liu, S., Beuerman, R. W. Tan, D. T. H., Tan, A. L., Liu, S. (2013). Rapid bactericidal action of alpha-mangostin against MRSA as an outcome of membrane targeting. *Biochimica et Biophysica Acta (BBA)-Biomembranes, 1828*(2), 834–844.

[59] Lakhani, S. A., & Bogue, C. W. (2003). Toll-like receptor signaling in sepsis. *Current Opinion in Pediatrics, 15*(3), 278–282.

[60] Low, A. G. (1982) The activity of pepsin, chymotrypsin and trypsin during 24 h periods in the small intestine of growing pigs. *British Journal of Nutrition, 48(1),* 147–159.

[61] Lyu, Y., Yang, Y., Lyu, X., Dong, N., & Shan, A. (2016) Antimicrobial activity, improved cell selectivity and mode of action of short PMAP-36-derived peptides against bacteria and Candida. *Scientific Reports, 6*, 27258.

[62] Lyu, Y., Yang, X., Goswami, S., Gorityala, B.K., Idowu, T., Domalaon, R., Zhanel, G.G., Shan, A., & Schweizer, F. (2017) Amphiphilic tobramycin-lysine conjugates sensitize multidrug resistant gram-negative bacteria to rifampicin and minocycline. *Journal of Medicinal Chemistry 60,* 3684–3702.

조선대학교
CHOSUN UNIVERSITY

[63] Ma, Z., Wei, D., Yan, P., Zhu, X., Shan, A., & Bi, Z. (2015). Characterization of cell selectivity, physiological stability and endotoxin neutralization capabilities of α-helix-based peptide amphiphiles. *Biomaterials, 52*, 517–530.

[64] Marín-Medina, N., Ramírez, D. A., Trier, S., & Leidy, C. (2016) Mechanical Properties That Influence Antimicrobial Peptide Activity in Lipid Membranes. *Applied Microbiology and Biotechnololgy*, *100(24)*, 10251−10263.

[65] Miyake, K. (2004). Endotoxin recognition molecules MD-2 and toll-like receptor 4 as potential targets for therapeutic intervention of endotoxin shock. *Current Drug Targets-Inflammation & Allergy, 3(3)*, 291−297.

[66] Moffatt, J. H., Harper, M., Mansell, A., Crane, B., Fitzsimons, T. C., Nation, R. L., Li, J., Adler, B., & Boyce, J. D. (2013). Lipopolysaccharide-deficient Acinetobacter baumannii shows altered signaling through host Toll-like receptors and increased susceptibility to the host antimicrobial peptide LL-37. *Infection and Immunity, 81(3)*, 684−689.

[67] Mookherjee, N., & Hancock, R. (2007). Cationic host defence peptides: innate immune regulatory peptides as a novel approach for treating infections. *Cellular and Molecular Life Sciences, 64(7-8)*, 922–933.

[68] Mueller, M., Lindner, B., Kusumoto, S., Fukase, K., Schromm, A. B., & Seydel, U. (2004). Aggregates are the biologically active units of endotoxin. *Journal of Biological Chemistry, 279(25)*, 26307–26313.

[69] Munford, R. S. (2005). Invited review: detoxifying endotoxin: time, place and person. *Journal of Endotoxin Research, 11(2),* 69–84.

[70] Nagaoka, I., Hirota, S., Niyonsaba, F., Hirata, M., Adachi, Y., Tamura, H., & Heumann, D. (2001). Cathelicidin family of antibacterial peptides CAP18

조선대학교
CHOSUN UNIVERSITY

and CAP11 inhibit the expression of TNF-α by blocking the binding of LPS to CD14+ cells. *The Journal of Immunology, 167(6)*, 3329–3338.

[71] Nan, Y. H., Bang, J.-K., Jacob, B., Park, I.-S., & Shin, S. Y. (2012). Prokaryotic selectivity and LPS-neutralizing activity of short antimicrobial peptides designed from the human antimicrobial peptide LL-37. *Peptides, 35(2)*, 239–247.

[72] Oren, Z., Shai, Y. (1998) Mode of Action of Linear Amphipathic α-Helical Antimicrobial Peptides. *Biopolymers, 47(6),* 451–463.

[73] Pollard. J. E., Snarr, J., Chaudhary, V., Jennings, J. D., Shaw, H., Christiansen, B., Wright, J., Jia, W., Bishop, R. E., Savage, P. B. (2012) In vitro evaluation of the potential for resistance development to ceragenin CSA-13. *Journal of Antimicrobial Chemotherapy, 67(11)*, 2665–2672.

[74] Rosenfeld, Y., Papo, N., & Shai, Y. (2006). Endotoxin (lipopolysaccharide) neutralization by innate immunity host-defense peptides peptide properties and plausible modes of action. *Journal of Biological Chemistry, 281(3)*, 1636–1643.

[75] Roth, B. L., Poot, M., Yue, S. T., & Millard, P. J. (1997) Bacterial viability and antibiotic susceptibility testing with SYTOX green nucleic acid stain. *Applied and Environmental Microbiology, 63(6)*, 2421–2431.

[76] Salazar, J., Alarcón, M., Huerta, J., Navarro, B., & Aguayo, D. (2017) Phosphoethanolamine addition to the Heptose I of the Lipopolysaccharide modifies the inner core structure and has an impact on the binding of Polymyxin B to the *Escherichia coli* outer membrane. *Archives of Biochemistry and Biophysics, 620*, 28–34.

[77] Sautrey, G., Zimmermann, L., Deleu, M., Delbar, A., Machado, L. S., Jeannot, K., Bambeke, F. V., Buyck, J. M., Decout, J-L., Mingeot-Leclercq,

조선대학교
CHOSUN UNIVERSITY

M.-P. (2014). New amphiphilic neamine derivatives active against resistant Pseudomonas aeruginosa and their interactions with lipopolysaccharides. *Antimicrobial Agents and Chemotherapy, 58(8)*, 4420–4430.

[78] Spohn, R., Daruka, L., Lázár, V., Martins, A., Vidovics, F., Grezal, G., Méhi, O., Kintses, B., Számel, M., Jangir, P. K., Csörgő, B., Györkei, A., Bódi, Z., Faragó, A., Bodai, L., Földesi , I., Kata, D., Maróti G., Pap, B., Wirth, R., Papp, B., & Pál, C. (2019) Integrated evolutionary analysis reveals antimicrobial peptides with limited resistance. *Nature Communication 10(1)*, 4538.

[79] Suzuki, K., Murakami, T., Kuwahara-Arai, K., Tamura, H., Hiramatsu, K., & Nagaoka, I. (2011). Human anti-microbial cathelicidin peptide LL-37 suppresses the LPS-induced apoptosis of endothelial cells. *International Immunology, 23(3)*, 185–193.

[80] van Langevelde, P., Kwappenberg, K. M., Groeneveld, P. H., Mattie, H., & van Dissel, J. T. (1998). Antibiotic-induced lipopolysaccharide (LPS) release from Salmonella typhi: delay between killing by ceftazidime and imipenem and release of LPS. *Antimicrobial Agents and Chemotherapy, 42(4)*, 739–743.

[81] Vianna, R. C., Gomes, R. N., Bozza, F. A., Amâncio, R. T., Bozza, P. T., David, C. M., & Castro-Faria-Neto, H. C. (2004). Antibiotic treatment in a murine model of sepsis: impact on cytokines and endotoxin release. *Shock, 21(2)*, 115–120.

[82] Vincent, J.-L., Pereira, A. J., Gleeson, J., & De Backer, D. (2014). Early management of sepsis. *Clinical and Experimental Emergency Medicine, 1(1)*, 3–7.

[83] Walsh, C. T., Wencewicz, T. A. (2014) Prospects for new antibiotics: a

조선대학교
CHOSUN UNIVERSITY

molecule centered perspective. *Journal of Antibiotis (Tokyo), 67(1)*, 7–22.

[84] Wang, J., Chou, S., Yang, Z., Yang, Y., Wang, Z., Song, J., Dou, X., Shan, A. (2018). Combating drug-resistant fungi with novel imperfectly amphipathic palindromic peptides. *Journal of Medicinal Chemistry, 61(9)*, 3889–3907.

[85] Wright, S. D., Tobias, P. S., Ulevitch, R. J., & Ramos, R. A. (1989) Lipopolysaccharide (LPS) Binding Protein Opsonizes LPS-bearing Particles for Recognition by a Novel Receptor on Macrophages. *Journal of Experimental Medicine*, *170(4)*, 1231–1241.

[86] Zhu, X., Zhang, L., Wang, J., Ma, Z., Xu, W., Li, J., & Shan, A. (2015). Characterization of antimicrobial activity and mechanisms of low amphipathic peptides with different α-helical propensity. *Acta Biomaterialia, 18*, 155–167.

조선대학교
CHOSUN UNIVERSITY

ACKNOWLEDDMENTS

저의 지도 교수님이신 존경하는 신송엽 교수님께 마음을 다해 감사하다는 말씀 전해드리고 싶습니다. 미운오리새끼 같았던 저를 품어 주시고 이끌어주셔서 정말 감사합니다.
교수님께서 부족한 저를 품어 주시지 않았다면 오늘의 저는 없었을 것입니다.
교수님 말씀 새기며 항상 생각하며 행동하는 연구자가 되겠습니다.
제 졸업 발표에 조언과 첨언을 아끼지 않으신 조승주 교수님, 양성태 교수님, 방정규 박사님, 이철원 교수님께 깊은 감사의 말씀 드립니다.
긴 시간 동안 제가 지치거나 힘들 때 마다 제 곁에서 힘이 되어주고 긍정에너지를 심어준 김인진언니, 이하나, 정상미, 김한나와 김미연에게도 고마운 마음을 전합니다.
그리고 사랑하는 가족이 있었기에 제가 힘든 시간 포기 하지 않고 이 자리에 있을 수 있었습니다. 못난 딸을 밤낮으로 늘 생각하며 저를 위해 기도해 주시며 아낌없이 베풀어주신 사랑하는 아버지 김영균 님과 어머니 표미숙님 그리고 늘 저를 예쁘게 봐주시고 물심양면으로 도와주신 사랑하는 아버님 박철호 님과 어머님 김용선 님께 고개 숙여 감사드립니다.
그리고 부족한 누나를 믿고 따라준 하나뿐인 동생 김기범에게도 감사의 인사를 전합니다.
박사 학위 동안 랩 생활을 하며 많은 의지가 되었던 랩 멤버인 Raja, Kumar, Ajish 에게도 감사의 인사를 전합니다.
같은 듯 다른 연구자의 길을 걷고 있는 또 다른 저의 우주인 남편 박상현님에게도 사랑하는 마음과 감사한 마음을 전합니다. 상현씨가 있기에 제가 있고 상현씨가 있기에 제가 무사히 박사과정을 끝낼 수 있었습니다.
고맙습니다. 앞으로도 잡은 손 놓지 말고 함께 쭉 걸어가요.
마지막으로 흐뭇한 표정으로 저를 내려다보고 계실 늘 그리운 사랑하는 할아버지께 부족하지만 제 눈물과 땀이 베어있는 이 논문을 바칩니다.